UCRL- 97285 Pt. 1
PREPRINT

UNSTABLE RADIATIVE-DYNAMICAL INTERACTIONS PART I: BASIC THEORY

Steven J. Ghan
Atmospheric and Geophysical Sciences Division
Lawrence Livermore National Laboratory
Livermore, California 94550

This paper was prepared for submission to
Journal of Atmospheric Sciences

June 1988

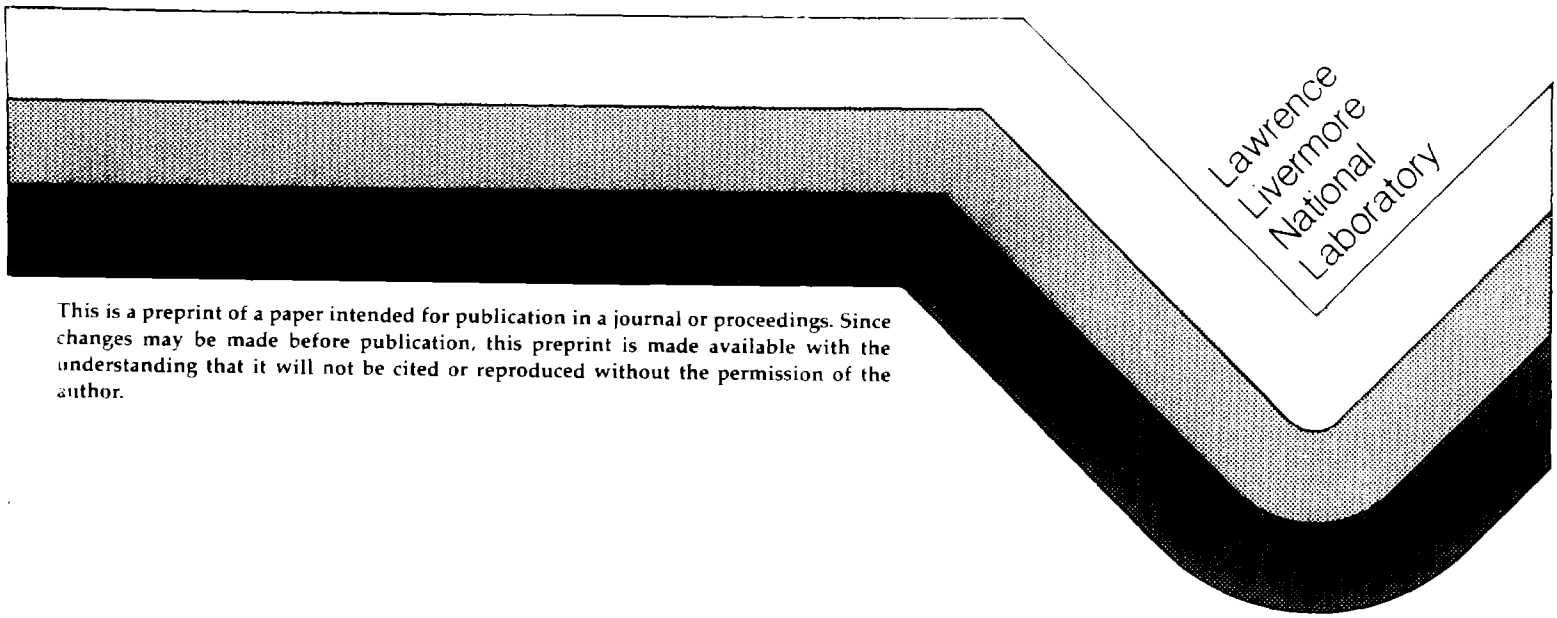

Abstract

The interaction between trace shortwave radiative absorbers and the dynamical circulation is shown to be linearly unstable for horizontally uniform basic states with a vertical gradient in the basic state absorber mixing ratio. Two types of instability are identified, described as the advective mode and the propagating mode. The advective mode is usually unstable when the basic state absorber mixing ratio decreases with height. Upward motion, high absorber concentration and warm temperatures are typically in phase for this mode. Growth rates, which can be competitive with those associated with baroclinic instability, are largest for perturbations that are much shorter than the internal deformation radius. Thus, the requirement that the basic state be horizontally uniform is often satisfied for the advective mode. The propagating mode is normally unstable when the basic state absorber mixing ratio increases with altitude. Propagating waves such as Rossby and inertia-gravity waves are amplified by the feedback with absorber transport and radiative heating. Growth rates for the propagating mode are usually bounded by the frequency of oscillation of the ambient wave, an important limitation for slowly propagating waves such as Rossby waves. Vertical transport of the absorber by the amplifying mode is down the basic state absorber mixing ratio gradient in each case.

1. Introduction

An outstanding feature of the terrestrial and Martian atmospheres is their near-transparency with respect to solar radiation. Although terrestrial water clouds scatter a significant fraction of the incoming solar radiation, and ozone absorbs much of the ultraviolet radiation, most absorption of visible radiation normally occurs at the surface. Radiative heating rates throughout most of the troposphere are dominated instead by infrared radiative cooling.

In the Martian atmosphere this situation is occasionally disrupted by global-scale dust storms, which increase the solar opacity of the atmosphere, leading to substantial tropospheric warming. Although such global storms fortunately do not develop in the Earth's atmosphere, recent numerical simulations (Malone et al., 1986) involving the terrestrial atmospheric response to massive injections of smoke produced by hypothetical post-nuclear war fires have exhibited a similar phenomenon. Substantial lofting of the smoke is found to occur in these simulations, suggesting that the feedback between shortwave radiative heating and the dynamical response to the heating can be important. The observed occurrence of Saharan dust storms (Westphal et al., 1987), lofting of smoke from forest fires, and evidence of increased atmospheric turbidity during glacial times all suggest that such interactions also occur locally in the Earth's atmosphere. Given the tendency of dust and soot to settle downward under the influence of gravity, the lofting mechanism associated with the absorption of solar radiation is clearly a key process in extending the duration and extent of dusty episodes.

The lofting mechanism is not a simple as one might expect. To illustrate this, Figure 1 shows the distribution of absorber mixing ratio thirty days following the injection of a Gaussian distribution centered at 10 km, as simulated by a two-dimensional slab-symmetric model on a midlatitude f-plane. One would expect

to find that the patch of absorber had risen from its level of injection, due to the circulation induced by the pressure gradients that develop from the horizontal heating gradient associated with the absorber patch. In fact we find little evidence of the patch-scale lofting because the horizontal scale of the absorber patch is so large (3000 km). Instead, we find that substantial lofting has occured on horizontal scales much smaller than the patch scale.The mechanism for this mode of lofting is quite different from that associated with the horizontal inhomogeneity of the patch, and will be the subject of this paper. Indeed, we shall find several distinct absorber transport mechanisms, each of which can be characterized as an unstable radiative-dynamical interaction.

The interaction between radiative heating, the dynamical circulation, and an absorber distribution has been investigated in several previous analytical studies. Lindzen (1966a,b) and Leovy (1966) examined the interaction between ozone and photochemical, shortwave radiative, and dynamical processes in the stratosphere and mesosphere. Gierasch et al. (1973) proposed an instability mechanism involving clouds, longwave radiation, and the dynamical circulation. Houben (1981) considered the interaction of Martian dust, solar radiation, and tidal circulations.

While these previous works represent important contributions to the specific problems that they address, there exists as yet no general theory of unstable radiative-dynamical interactions. The work of Lindzen (1966a,b) and Leovy (1966) specifically includes photochemical processes that, though important for ozone, do not apply to aerosols. The theory developed by Geirasch et al. (1973) is restricted to constituents that are important only for infrared radiation. Leovy et al. (1973), Leovy and Zurek (1979), and Schneider (1983) discuss mechanisms for the interaction of solar heating and transport of dust, but never explicitly represent the dust transport. Houben (1981) treats dust transport, but only horizontally. Haberle et al. (1982), Haberle et al. (1985), and Malone et al. (1986) treat the vertical

transport of the absorber, but resort to numerical means to do so. Given the similarities in the coupling between the dynamical circulation and Martian dust, stratospheric ozone, volcanic aerosols, tropospheric dust and smoke, and any other shortwave radiative absorber, what is clearly needed is a general theory for the unstable interaction between the absorber and the dynamical circulation. This paper represents an attempt to develop just such a theory.

As in other instability theories, only modal (i.e., exponentially amplifying) instabilities shall be considered in the theory. Thus, lofting of the absorber due simply to an initial horizontal inhomogeneity in its distribution will be excluded from the initial analysis. While such nonmodal lofting can be important for absorber patches of limited horizontal scale, it is not as amenable to analysis as is the modal instability. The obvious question of which form of lofting, modal or nonmodal, is more important shall be addressed in Ghan and Covey (1988) using a combination of numerical simulations and simple physical arguments.

For clarity the present theory is developed under a variety of simplifying approximations. However, the general procedure is the same in each case. In particular, the radiative heating is first expressed in terms of an absorber mixing ratio. The equations governing conservation of mass, momentum, potential temperature and absorber mixing ratio are then linearized about a horizontally uniform basic state. The linear system of equations is then reduced to a single partial differential equation (PDE). By expressing solutions in terms of orthogonal basis functions with a time dependence given by $\exp(-i\sigma t)$, the PDE reduces to an algebraic equation for σ. Solutions are unstable if $Im(\sigma) > 0$.

An important parameter that emerges from the analysis is the rate of radiative-dynamical feedback, defined as

$$\alpha \equiv -\frac{RS_0 a\overline{T}}{c_p N^2 H}\frac{\partial \overline{q}}{\partial z} \tag{1.1}$$

where S_0 is the solar constant, $\bar{q}$ is the basic state absorber mass mixing ratio, a is the specific absorption coefficient for the absorber, and

$$\overline{T}(z) = \exp\left(-\frac{1}{\mu}\int_z^\infty a\rho_0\bar{q}dz'\right) \tag{1.2}$$

is the basic state transmissivity between the top of the atmosphere and level z. The remaining symbols take their standard meteorological meaning, as defined in Appendix A. One interpretation of α is that α^{-1} represents the time scale in which perturbations in absorber mixing ratio, through vertical advection induced by radiative heating, feed back upon themselves. In many instances the growth rate of unstable disturbances is, in the absence of dissipation, proportional to α; in most cases the growth rate does not exceed the feedback rate. Thus, the radiative-dynamical feedback rate characterizes the growth rate. By determining limits to the feedback rate, we can place an upper bound on the growth rate.

For example, if we assume that $\bar{q}(z)$ decreases exponentially with scale height h, then for grey absorption

$$a\frac{\partial\bar{q}}{\partial z} = -a\bar{q}/h = -\frac{\tau_a}{\rho_0}\frac{H-h}{Hh^2} \tag{1.3}$$

where

$$\tau_a(z) = \int_z^\infty a\rho_0\bar{q}dz' \tag{1.4}$$

is the absorption optical depth from the top of the atmosphere to level z. The feedback rate then becomes

$$\alpha = \alpha_0\frac{H}{h}\left(1+\frac{H}{h}\right)\tau_a\exp\left(-\frac{\tau_a}{\mu}\right) \tag{1.5}$$

where

$$\alpha_0 = \frac{RS_0}{c_p\rho_0N^2H^3} \simeq 4\times10^{-6}\mathrm{s}^{-1} \tag{1.6}$$

for $\rho_0 = 1$ kg m^{-3}, $S_0 = 1360$ Wm^{-2}, $N = 10^{-2}$s^{-1}, and $H = 10$ km. At sufficiently high altitudes, where $\tau_a \ll \mu$, the transmissivity is near unity but the absorber

gradient is small, so the feedback rate is small. In optically thick atmospheres ($\tau_a \gg 1$), the absorber gradient is large near the surface but the transmissivity is small, so the feedback rate is again small. However, at the altitude for which $\tau_a = \mu$ the feedback rate for a given $\bar{q}(z)$ is a maximum, given by

$$\alpha_{\max} = 0.37\ \alpha_0\ \mu \frac{H}{h}\left(1 - \frac{H}{h}\right) \quad . \tag{1.7}$$

For $\mu = 1$ (i.e., summertime at local noon), maximum values are

$$\alpha_{\max} = \begin{cases} (4\text{ days})^{-1} & \text{for } h = H = 10\text{ km} \\ (1.7\text{ hrs})^{-1} & \text{for } h = H/10 = 1\text{ km} \end{cases} \quad . \tag{1.8}$$

Thus, if the absorption optical depth exceeds unity and the vertical gradient of absorber mixing ratio is large enough, the radiative-dynamical feedback rate in the summer hemisphere (i.e., when solar radiation is strong) can be quite strong. Growth rates of unstable modes can be competitive with those associated with baroclinic instability.

The physical mechanism for the instability depends on whether the basic state absorber mixing ratio increases or decreases with altitude. If the basic state absorber mixing ratio decreases with altitude, then upward motion increases the local absorber concentration. Assuming radiative heating increases with increasing local absorber concentration, the upward motion increases the radiative heating, leading to warming. If the perturbation is to amplify, warm temperatures must be positively correlated with the upward motion. To maximize the conversion of potential energy to kinetic energy, warm temperatures should be perfectly correlated with the upward motion. In this instance, this occurs if the frequency of oscillation is much less than the growth rate. As illustrated in Figure 2, upward motion, high absorber concentration, radiative heating, and warm temperatures all coincide. This unstable mode we shall term the advective mode, since propagation for this mode is weak; indeed, the mode does not propagate at all in the limit of zero radiative-dynamical feedback.

If, on the other hand, the basic state absorber mixing ratio increases with altitude, then the advective mode is damped. However, as we shall demonstrate, propagating Rossby and inertia-gravity waves can amplify. If the frequency of oscillation is much larger than the growth rate, then high absorber concentrations, and hence strong radiative heating, lags downward motion by one quarter cycle, and lead warm temperatures by one quarter cyle. Thus, warm temperatures are again positively correlated with upward motion. Potential energy is converted to kinetic energy, and the perturbation amplifies. This mechanism was first described by Leovy (1966). Figure 2 also illustrates the phase relation for this type of instability, which we shall term a propagating instability because it relies on propagation for the proper phase relation of heating, temperature, and vertical motion. Note that the growth rate for the propagating instability must be much less than the frequency of oscillation, a significant constraint for slowly propagating waves when the radiative-dynamical feedback rate is strong.

The remainder of this paper shall describe various aspects of the radiative-dynamical interaction in considerably greater detail. Section 2 discusses the representation of the radiative heating in terms of the absorber mixing ratio. In section 3 the theory is developed using the quasi-geostrophic approximation for uniform radiative-dynamical feedback; the theory is generalized to the primitive equations on an f-plane and on a β-plane in section 4. Distributions of absorber mixing ratio that are consistent with uniform radiative-dynamical feedback are determined in section 5. Complicating factors such as dissipation, vertical shear, and scattering, which are neglected in the present paper, are treated in Ghan(1988b). The conclusions are summarized in section 6.

The development of the theory of radiative-dynamical interaction is intentionally general, with relatively few references to specific examples of physical phenomena. This approach is taken to permit the exploration of a wide range of values in

parameter space, and hence broaden our understanding of the radiative-dynamical interaction. Indeed, numerous surprising aspects of the interaction are discovered which might have been overlooked in a more specialized investigation.

2. Parameterization of Radiative Heating

The first step in developing a theory of radiative-dynamical instability is to express the shortwave radiative heating in terms of the absorber distribution. Here we do so under the assumption that scattering can be neglected and that absorption is grey (i.e., independent of wavelength in the solar spectrum). Although the first assumption is not strictly true for most aerosols, calculations discussed in Ghan (1988b) demonstrate little sensitivity to the fraction of sunlight scattered. The grey approximation is reasonable for many aerosols but is inaccurate for most gaseous absorbers. However, nongrey effects can be treated with little loss of generality.

In the absence of scattering, the shortwave radiative heating at a level z can be expressed, under the grey approximation, as

$$Q(z) = -\frac{\partial F}{\partial z} = \mu S_0 \frac{\partial}{\partial z} \exp\left(-\frac{1}{\mu}\int_z^\infty a\rho_0 q dz'\right) = S_0 a \rho_0 q(z) T(z) \qquad (2.1)$$

where S_0 is the solar constant, μ is the cosine of the solar zenith angle, a is the specific absorption coefficient, q is the absorber mass mixing ratio, and

$$T(z) = \exp\left(-\frac{1}{\mu}\int_z^\infty a\rho_0 q dz'\right) \qquad (2.2)$$

is the atmospheric transmissivity. For small perturbations about a stratified $\bar{q}(z)$,

$$Q' \simeq S_0 a \rho_0 \left(\bar{T} q' - \bar{q} T'\right) \qquad (2.3)$$

unless $\mu < 0$, in which case $Q' = 0$.

The first term in (2.3) represents the dependence of the local perturbation heating rate on the local perturbation absorber concentration. The second term represents the dependence of the heating on the absorption above the reference level. If, for example, an absorber perturbation has a sufficiently deep vertical distribution, the reduction in the transmissivity due to high absorber concentrations

aloft can reduce or even dominate the enhanced heating associated with high local absorber concentrations. Such perturbations in transmissivity, then, are potentially important and hence should be treated. However, in the development of the basic theory presented here we shall in the interest of simplicity neglect perturbations in transmissivity. Then the parameterization of the perturbation heating reduces to

$$Q' \simeq S_0 a \rho_0 \overline{T} q'. \tag{2.4}$$

For a discussion of the effect of perturbations in transmissivity on the radiative-dynamical interaction, and the conditions under which it is important, see the companion paper (Ghan, 1988b).

3. Quasi-Geostrophic Stability Analysis

The essential aspects of the radiative-dynamical instability can be demonstrated most easily within the context of the quasi-geostrophic theory. In this section we present an illustrative solution of the instability, or eigenvalue, problem under a number of somewhat restrictive assumptions. These include, in addition to the quasi-geostrophic approximation, the assumptions of a horizontally uniform basic state, no vertical shear in the basic state flow, no dissipation (or, at least, the same uniform damping rate for all dependent variables), and uniform Brünt-Vaisala frequency and radiative-dynamical feedback rate. The generalization to the primitive equations is considered in section 4; the effects of vertical shear, dissipation, and nonuniform radiative-dynamical feedback are addressed in Ghan (1988b).

Consider the linearized quasi-geostrophic equations governing the conservation of vorticity ζ, and potential temperature θ, which for log-pressure coordinates can be written

$$D\zeta - \beta v = f_0 \frac{1}{\rho_0}\frac{\partial}{\partial z}(\rho_0 w) \tag{3.1}$$

$$D\theta = -\frac{\partial \bar{\theta}}{\partial z} w + Q/(Ec_p\rho_0) \tag{3.2}$$

where

$$D = \frac{\partial}{\partial t} + \bar{u}\frac{\partial}{\partial x} + \epsilon \tag{3.3}$$

is the linearized advection and damping operator, and $E = (p/p_0)^\kappa$ is the Exner function. The remaining symbols are defined in Appendix A.

In quasi-geostrophic theory, the horizontal velocity can be expressed in terms of a streamfunction ψ,

$$v = \frac{\partial \psi}{\partial x} \tag{3.4}$$

$$\zeta = \nabla^2 \psi \tag{3.5}$$

and the potential temperature follows from the hydrostatic relation

$$\theta = \frac{f_0 H}{RE} \frac{\partial \psi}{\partial z} \quad . \tag{3.6}$$

Substituting (3.4)-(3.6) into (3.1)-(3.2), the conservation equations for vorticity and potential temperature become

$$\left(D\nabla^2 + \beta \frac{\partial}{\partial x} \right) w = f_0 \frac{1}{\rho_0} \frac{\partial}{\partial z}(\rho_0 w) \tag{3.7}$$

$$f_0 D \frac{\partial \psi}{\partial z} = -N^2 w + RQ/(c_p \rho_0 H) \quad . \tag{3.8}$$

Solving (3.7) and (3.8) for the vertical velocity w yields the Rossby wave equation

$$f_0^2 \frac{\partial}{\partial z} \frac{1}{\rho_0} \frac{\partial}{\partial z}(\rho_0 D w) + \left(D\nabla^2 - \beta \frac{\partial}{\partial x} \right) \left[N^2 w - RQ/(c_p \rho_0 H) \right] = 0 \tag{3.9}$$

where we have assumed $\bar{u}$ and hence D does not vary with altitude (this constraint is relaxed in Ghan, 1988b).

The feedback between the radiative heating Q and the dynamical circulation w is treated by expressing the heating in terms of a shortwave radiative absorber mixing ratio q and then relating the absorber concentration to the circulation. Combining (2.4) and (3.9), the Rossby wave equation then becomes

$$f_0^2 \frac{\partial}{\partial z} \frac{1}{\rho_0} \frac{\partial}{\partial z}(\rho_0 D w) - \left(D\nabla^2 + \beta \frac{\partial}{\partial x} \right) \left(N^2 w - \frac{RS_0 a \bar{T} q'}{c_p H} \right) = 0 \quad . \tag{3.10}$$

The linearized equation governing conservation of absorber can be similarly expressed, assuming a horizontally uniform basic state absorber distribution,

$$Dq' = -\frac{\partial \bar{q}}{\partial z} w \quad . \tag{3.11}$$

Eliminating q' between (3.10) and (3.11) yields the PDE

$$\frac{f_0^2}{N^2} \frac{\partial}{\partial z} \frac{1}{\rho_0} \frac{\partial}{\partial z}(\rho_0 D^2 w) - (D\nabla^2 - \beta \frac{\partial}{\partial x})(D - \alpha) w = 0 \tag{3.12}$$

where

$$\alpha \equiv -\frac{RS_0 a\overline{T}}{c_p N^2 H}\frac{\partial \overline{q}}{\partial z} \tag{3.13}$$

is defined to be the rate of radiative-dynamical interaction. As we shall see, the magnitude of α characterizes the growth rate of unstable solutions of (3.12).

We shall now assume that the coefficients of (3.12) are constant (density is assumed to vary with a constant scale height H). This permits plane-wave solutions, which greatly simplifies the analysis. While such an assumption is common and often justifiable for the Brünt-Vaisala frequency, it is not necessarily reasonable for the radiative-dynamical feedback rate α. The effects of treating variations in the feedback rate are discussed in Ghan (1988b).

Assuming N^2 and α are independent of height, normal mode solutions of the form

$$w(x,y,z,t) = w_0 \exp(z/2H) \exp[i(kx - \ell y + mz - \sigma t)] \tag{3.14}$$

yield the algebraic relation

$$\frac{f_0^2}{N^2} n^2 D^2 + (k_2^2 D - ik\beta)(D - \alpha) = 0 \tag{3.15}$$

where

$$n^2 = m^2 + \frac{1}{4H^2} \tag{3.16}$$

$$k_2^2 = k^2 - \ell^2 \quad . \tag{3.17}$$

Solutions satisfying the proper boundary conditions are unstable provided $Im(\sigma) > 0$. Because

$$D = -i\sigma - \overline{u}ik - \epsilon \tag{3.18}$$

for such waves, this is equivalent to the condition that the real part of D exceeds ϵ.

In addition to satisfying the dispersion relation (3.15), solutions must also satisfy the boundary conditions, which are

$$w(0) = 0 \tag{3.19a}$$

$$\rho_0 w\psi \text{ bounded as } z \to \infty \tag{3.19b}$$

The lower boundary condition determines the vertical phase of solutions. For an atmosphere with a finite top, the upper boundary condition leads to the restriction that only a discrete set of vertical wavenumbers is permitted. For an infinite atmosphere, this quantization does not apply. Note that downward energy propagation is permitted due to energy released by the instability at higher levels.

We shall now consider solutions to (3.15). Although the solutions can be expressed analytically, the expressions are complicated and not particularly meaningful. We shall instead consider several limiting cases.

In the first case the magnitude of the feedback rate is much less than the frequency of internal Rosssby waves, i.e.,

$$\alpha \ll k\beta/k_3^2 \tag{3.20}$$

where

$$k_3^2 = k_2^2 - \frac{f_0^2}{N^2}\, n^2 \quad . \tag{3.21}$$

Approximate solutions of (3.15) are

$$D \simeq \frac{i\beta k}{k_3^2} - \alpha\frac{f^2 n^2}{N^2 k_3^2} \quad , \quad \alpha - \frac{i\alpha^2 k_3^2}{\beta k}\,\frac{f^2 n^2}{N^2 k_3^2} \quad . \tag{3.22}$$

The first solution corresponds to an internal Rossby wave which propagates westward with respect to the mean flow but, in the absence of radiative-dynamical feedback ($\alpha = 0$), does not amplify. The second solution corresponds to the advective mode which, in the absence of feedback, neither propagates nor grows. If

$S_0 a\overline{T} \neq 0$ but $\bar{q}_z = 0$, the two solutions correspond to (a) the absorber being simply advected by the mean flow, forcing vertical motion through radiative heating, and driving a circulation through vortex stretching, and (b) no absorber perturbation, with Rossby waves propagating freely; if, on the other hand, $\bar{q}_z \neq 0$ but $S_0 a\overline{T} = 0$, the solutions correspond to (a) Rossby waves propagating freely, advecting the absorber, and (b) the absorber simply advected by the mean flow, with no perturbation circulation.

In the presence of positive radiative-dynamical feedback ($\alpha > 0$, i.e., absorber mixing ratio decreasing with altitude), the Rossby mode is damped but the advective mode will amplify. The growth rate of the advective mode is approximately equal to the feedback rate, and hence for spatial scales that satisfy (3.20) the growth rate is independent of the spatial scales of the purturbation. In addition, because $\alpha \ll k\beta/k_3^2$ for this case and $f^2 n^2 \ll N^2 k_3^2$ in general, one can readily show that the growth rate of the advective mode dominates the frequency of oscillation (which, incidently, indicates weak eastward propagation). Thus, the perturbation heating and vertical velocity are in phase, with upward motion coinciding with high absorber concentrations and temperatures.

In the presence of negative radiative-dynamical feedback ($\alpha < 0$, i.e., absorber mixing ratio increasing with height), the advective mode is damped but the Rossby mode is unstable. The growth rate of the Rossby mode is largest for perturbations that are long and shallow (i.e., $k_z^2 \ll f^2 n^2/N^2$, which holds for horizontal scales much longer than the internal deformation radius), with the maximum growth rate approximately equal to the feedback rate which for this case is also much smaller than the Rossby wave frequency. Thus, in contrast to the advective mode for positive feedback, the growth rate of the Rossby mode for this case is much smaller than the frequency of oscillation. Although the perturbation vertical velocity and temperature are in phase for both the unstable advective mode and the unstable

Rossby mode, the perturbation heating and vertical velocity are in phase for the advective mode but they are nearly 90° out of phase for the Rossby mode. In terms of energetics, both unstable modes amplify by generating available potential energy (APE) through radiative heating (i.e., $\overline{Q'\theta'} > 0$) and then converting the APE to kinetic energy (i.e., $\overline{w'\theta'} > 0$), but the energy generation process is less efficient for the Rossby mode because the phase difference between the heating and temperature is nearly 90°.

For both positive and negative radiative-dynamical feedback the unstable mode transports the absorber down the gradient of mean absorber mixing ratio. That is, from the absorber balance the vertical transport

$$\overline{w'q'} = Re\left(-\frac{1}{D}\right)\frac{\partial\bar{q}}{\partial z}\,|w|^2 = -\frac{D_r}{D_r^2 - D_i^2}\,\frac{\partial\bar{q}}{\partial z}\,|w|^2 \qquad (3.23)$$

is upward (downward) if the mean absorber mixing ratio decreases (increases) with altitude. Thus, the unstable modes reduce the magnitude of the absorber gradient, and hence reduce the instability of the radiative-dynamical system. The unstable modes will continue to disperse the absorber distribution until the feedback mechanism is too weak to overcome the dissipative processes. Given (3.23) and simple (or the more accurate general analytical) solutions such as (3.21) for the growth rate and frequency, it may be possible to develop parameterizations for the absorber transport in terms of the basic state variables. However, a plausible closure assumption for the perturbation amplitude $|w|^2$ and a scale selection criterion are required.

In the second limiting case we assume that

$$\frac{\beta k}{k_2^2}\,\frac{k_3^2}{k_2^2} \ll \alpha \ll f \quad . \qquad (3.24)$$

The lower bound is greater than the Rossby wave frequency for all wave scales. The upper bound follows from subsequent consideration of the primitive equations in

section 4. Note that implicit in (3.24) is the assumption that the Coriolis frequency exceeds the Rossby wave frequency. While this is true for synoptic scale waves in midlatitudes, it is not true for planetary waves in midlatitudes or for all waves near the equator. Thus, the present case is restricted to sub-planetary scales in mid-latitudes. Approximate solutions of (3.15) for this case are

$$D \simeq \frac{i\beta k}{k_2^2} - \frac{\beta^2 k^2}{\alpha}\frac{f^2 n^2}{N^2 k_2^6} \quad , \quad \frac{\alpha k_3^2}{k_3^2} - \frac{i\beta k}{k_3^2}\frac{f^2 n^2}{N^2 k_2^2} \quad . \tag{3.25}$$

The first solution again corresponds to the Rossby mode, while the second solution represents the advective mode.

In the presence of positive radiative-dynamical feedback ($\alpha > 0$), the advective mode is again unstable, but with the growth rate somewhat less than the feedback rate. The growth rate for this case depends on the spatial scales of the perturbation, increasing with decreasing horizontal scale and increasing vertical scale. In particular, the growth rate is largest for waves with horizontal scales much less than the internal deformation radius, i.e., for scales such that $k_2^2 \sim k_3^2 \gg f^2 n^2 / N^2$. For all perturbation scales that satisfy the condition (3.24), one can show that the growth rate of the advective mode again dominates the frequency of oscillation (which again indicate weak eastward propagation).

In the presence of negative radiative-dynamical feedback ($\alpha < 0$), the Rossby mode is unstable. The most notable feature of the approximate solution (3.25) for the Rossby mode is that when the feedback is strong such that condition (3.24) is satified, the growth rate of the Rossby mode actually decreases as the feedback rate increases in magnitude. This is in contrast to the case with weak feedback, in which the growth rate of the Rossby mode increases with the magnitude of the feedback rate. Thus, for a given perturbation scale (k, l, m), the growth rate of the Rossby mode is largest for an intermediate feedback rate. Although we cannot demonstrate it analytically, the feedback rate at which the Rossby mode growth

rate is largest appears to be near the transition frequency between cases (3.20) and (3.24), i.e.,

$$\alpha_m \equiv -\frac{\beta k}{k_2^2} \frac{k_3^2}{k_2^2} \quad . \tag{3.26}$$

The scale dependence of the Rossby mode growth rate is fairly complicated. For this reason we shall defer discussion of the scale dependence until section 4, in which the dependence is illustrated graphically.

In summary, we have found through a number of simplifying approximations that unstable radiative-dynamical interactions are possible when absorber mixing ratio increases or decreases with height. The physical mechanisms for the instability in the two cases are quite different, but also exhibit some similarities. We have derived some approximate expressions for the complex eigenfrequencies in several special cases. These and other expressions are summarized in Table 1. Many of the assumptions required for the analysis in this illustrative analysis are relaxed in the following section and in Ghan (1988b). Many of the basic conclusions are, however, unaltered by the additional considerations.

4. Generalization to the Primitive Equations

The theory developed so far has been restricted by the quasi-geostrophic approximation, which filters out the inertia-gravity modes. Moreover, we shall find that the quasi-geostrophic solution of the advective mode is inaccurate when the rate of radiative-dynamical feedback exceeds the Coriolis frequency. To apply the theory to the inertia-gravity modes, and to cases in which the feedback rate exceeds the Coriolis frequency, the theory must be extended to the primitive equations.

Linearizing about a horizontally uniform basic state, the primitive equations in log-pressure coordinates can be written

$$Du - fv = -\frac{\partial \Phi}{\partial x} \tag{4.1}$$

$$Dv + fu = -\frac{\partial \Phi}{\partial y} \tag{4.2}$$

$$\frac{\partial u}{\partial x} + \frac{\partial v}{\partial y} + \frac{1}{\rho_0}\frac{\partial}{\partial z}(\rho_0 w) = 0 \tag{4.3}$$

$$D\frac{\partial \Phi}{\partial z} = -N^2 w + \frac{RQ}{c_p \rho_o H} \quad . \tag{4.4}$$

The solution on a β-plane is much more complicated than on an f-plane. Because inertia-gravity waves are insensitive to the β term, we shall first consider the solution for a midlatitude f-plane.

a. Midlatitude f-Plane

On an f-plane, the Coriolis parameter is assumed to be constant. Assuming the advective operator D is uniform, the primitive equations can then be reduced to a single partial differential equation for the vertical velocity,

$$(D^2 + f_0^2)D\frac{\partial}{\partial z}\frac{1}{\rho_0}\frac{\partial}{\partial z}(\rho_0 w) + D\nabla^2(N^2 w - \frac{RQ}{c_p \rho_0 H}) = 0 \tag{4.5}$$

This wave equation differs from the Rossby wave equation (3.9) because of the presence of the D^2 term and the absence of a β-term.

Combining (4.5) with the heating expression (2.4) and the absorber budget equation (3.11) yields the PDE

$$(D^2 + f_o^2)D\frac{\partial}{\partial z}\frac{1}{\rho_o}\frac{\partial}{\partial z}(\rho_o w) + N^2\nabla^2(D - \alpha)w = 0 \qquad (4.6)$$

where the radiative-dynamical feedback rate α is defined by (3.13). Assuming N, α and the density scale height H are constant, normal mode solutions of the form (3.14) yield the algebraic relation

$$(D^2 - f_0^2)Dn^2 - N^2k_2^2(D - \alpha) = 0 \quad . \qquad (4.7)$$

In the absence of radiative-dynamical feedback ($\alpha = 0$), solutions to (4.7) are

$$D = 0, \pm i\frac{Nk_3}{n} \qquad (4.8)$$

which correspond to the advective and eastward- and westward-propagating inertia-gravity modes.

In the presence of feedback, solutions to (4.7) are more complicated. We shall therefore consider approximate solutions in some limiting cases, corresponding to whether the magnitude of the radiative-dynamical feedback rate is much greater than or much less than a scale-dependent parameter

$$\gamma \equiv \frac{2Nk_3^3}{3\sqrt{3}\,nk_2^2} \quad . \qquad (4.9)$$

For waves that are either long and shallow ($f^2n^2 \gg N^2k_2^2$) or short and deep ($f^2n^2 \ll N^2k_2^2$), it can be shown that γ is much larger than the Coriolis frequency. For waves with an intermediate aspect ratio ($f^2n^2 = N^2k_2^2$) γ is of the same order as the Coriolis frequency. Thus, γ is larger than or of the same order as f for all wave scales.

In the first case, we assume weak radiative-dynamical feedback, i.e., $|\alpha| \ll \gamma$. If $|\alpha \ll f$, this condition is assured for all waves scales. Then approximate solutions to (4.7) are

$$D \simeq \frac{\alpha k_2^2}{k_3^2} \quad , \quad \simeq -\frac{iNk_3}{n} - \frac{\alpha k_2^2}{2k_3^2} \qquad (4.10)$$

which correspond to the advective mode and the eastward and westward propagating inertia-gravity waves, respectively.

In the presence of positive radiative-dynamical feedback ($\alpha > 0$, i.e., absorber mixing ratio decreasing with altitude), the two inertia-gravity modes are damped by the feedback, while the advective mode amplifies in the absence of dissipation. In fact, the expression for the growth rate of the advective mode agrees exactly with the approximate quasi-geostrophic solution (3.25) when the feedback rate is much larger than the internal Rossby wave frequency. Thus, we conclude that the quasi-geostrophic solution is accurate for all scales if the feedback rate is less than the Coriolis frequency. Even for feedback rates greater than f, the quasi-geostrophic solution is accurate for waves that are sufficiently short and deep or sufficiently long and shallow that $|\alpha| \ll$ [illegible]. Note that the oscillation frequency of the advective mode vanishes for the present case because we have assumed an f-plane rather than a β-plane.

In the presence of negative radiative-dynamical feedback ($\alpha < 0$, i.e., absorber mixing ratio increasing with altitude), the advective mode is damped, while both inertia-gravity modes are unstable in the absence of dissipation. The scale-dependence of the growth rate of the unstable inertia-gravity modes is identical to that of the unstable advective mode, except that the growth rate of the inertia-gravity modes is one half that of the advective mode for the same feedback magnitude. As with the Rossby waves on the β-plane, the growth rate of the unstable inertia-gravity waves can be shown to be much less than the frequency of oscillation. Thus, the inertia-gravity waves will have a phase structure similar to that of the unstable Rossby waves. Leovy (1966) first discussed the physical mechanism of this mode of instability, in the context of the photochemistry of oxygen in the lower mesosphere.

For strong radiative-dynamical feedback ($|\alpha| \gg \gamma$), approximate solutions to (4.7) are

$$D \simeq \alpha \left(\frac{N^2 k_2^2}{\alpha^2 n^2} \right)^{1/3} \quad , \quad -\alpha \, \frac{1 \pm i\sqrt{3}}{2} \left(\frac{N^2 k_2^2}{\alpha^2 n^2} \right)^{1/3} \quad . \tag{4.11}$$

In the presence of positive feedback ($\alpha > 0$), the advective mode is again non-propagating and, in the absence of dissipation, unstable. However, the growth rate increases much more slowly with increasing feedback. In particular, the growth rate is proportional to the feedback rate to the one-third power. Moreover, the scale dependence of the growth rate is different from the cases with weaker feedback. The growth rate increases with the vertical scale of the wave, even for waves that are short and deep, and decreases as the horizontal scale increases, even for waves that are long and shallow. For all waves scales for which $|\alpha| \gg \gamma$, however, the growth rate of the advective mode is much less than the feedback rate, and is less than the quasi-geostrophic solution.

In the presence of negative radiative-dynamical feedback ($\alpha < 0$), the inertia-gravity modes are again unstable in the absence of dissipation. The growth rate of the inertia-gravity modes is again equal to one-half that of the unstable advective mode for the same feedback magnitude. The frequency of oscillation of the inertia-gravity modes is greatly increased by the feedback, but is only slightly larger than the growth rate.

Table 1 summarizes the approximate expressions for the complex eigenfrequency derived here, along with those derived in section 3.

b. β-plane

We have seen that for the advective mode the latitudinal variation of the Coriolis parameter must be accounted for if $|\alpha| \leq \beta k / k_3^2$. We have also seen that the primitive equations may be required if $|\alpha| \geq f$. If $f > \beta k / k_3^2$ then $|\alpha|$ cannot be

both less than $\beta k/k_3^2$ and greater than f, so that the previous analyses are sufficient to cover all possible feedback rates. However, if $f < |\alpha| < \beta k/k_3^2$ the foregoing analyses are inapplicable. In this case it is necessary to treat the primitive equations on a β-plane, if not a sphere. In midlatitudes, the condition $f < \beta k/k_3^2$ is met for the planetary scales (for which spherical geometry is required regardless of the feedback rate); in the subtropics and tropics, f may be less than $\beta k/k_3^2$ for a variety of spatial scales.

Here we shall consider the radiative-dynamical feedback for the primitive equations on β-planes. Two cases will be considered, namely a midlatitude β-plane, for which $f < \beta k/k_3^2$ for the planetary scales, and an equatorial β-plane, for which $f < \beta k/k_3^2$ for nearly all spatial scales.

In either case, accounting for the latitudinal variation of the Coriolis parameter greatly complicates the analysis. In the absence of radiative-dynamical feedback, the classical β-plane theory of waves (Lindzen, 1967) reduces the linearized primitive equations to a single equation for the meridional rather than vertical velocity: solutions for which $v = 0$ are treated separately. We shall take the same approach here. The resulting wave equation with radiative-dynamical feedback can be written

$$\left(D^2 - f^2\right) D^2 \frac{\partial}{\partial z} \frac{1}{\rho_0} \frac{\partial}{\partial z} (\rho_0 v) + N^2 \left(D\nabla^2 - \beta \frac{\partial}{\partial x}\right) (D - \alpha) v = 0 \quad . \qquad (4.12)$$

For the midlatitude case it is sufficient to treat f and β as constants in (4.12): this approximation is not reasonable for the equatorial β-plane. Because this distinction alters the analysis considerably, we shall consider the midlatitude and equatorial cases separately.

On a mid-latitude β-plane f and β are treated as constants in (4.12). Then the usual Fourier basis functions given by (3.14) are sufficient to reduce the problem

to an algebraic equation, namely,

$$\frac{n^2}{N^2} D^4 - k_3^2 D^2 - \left(\alpha k_2^2 + ik\beta\right) D - i\alpha k\beta = 0 \quad . \tag{4.13}$$

This quartic equation for D admits four solutions, corresponding to the advective mode, the Rossby mode, and two inertia-gravity modes. We have discussed these modes in the previous analyses of the quasi-geostrophic system on a midlatitude β-plane and the primitive equations on an f-plane. For synoptic and mesoscales in midlatitudes, those treatments covered all possible cases except for the inertia-gravity modes on a β-plane and the Rossby mode when the feedback rate exceeds the Coriolis frequency. Here we shall consider those cases and solutions when the feedback rate does not satisfy any of the special limiting cases. Although one can express exact solutions to (4.13) analytically, the expressions are not meaningful, and hence will not be presented. Rather, we shall present the analytical solutions graphically, thereby illustrating the parametric dependence of the growth rate for parameter ranges that do not admit simple solutions.

The advective mode is unstable for positive radiative-dynamical feedback, i.e., absorber decreasing with altitude. Figure 3 shows the advective mode growth rate, normalized by the feedback rate, as a function of the feedback rate, for zonal and meridional wavelengths of 1000 km, and a vertical wavelength of 10 km. Three different parameter regimes are evident in this figure. For feedback rates much smaller than the internal Rossby wave frequency (8×10^{-7} s^{-1} for the wave scale assumed in Figure 3), the growth rate is, consistent with (3.22), nearly equal to the feedback rate. For feedback rates much larger than the Rossby wave frequency but much smaller than the Coriolis frequency (10^{-4} s^{-1}), the growth rate is again approximately proportional to the feedback rate, but with the constant of proportionality less than one. Consistent with (3.25) and (4.10), the constant is k_2^2/k_3^2, or 0.67 for the wave scale assumed in Figure 3. For feedback rates much greater

than the Coriolis frequency, the growth rate increases more slowly than the feedback rate. In particular, according to (4.11), the growth rate increases with the feedback rate to the one-third power in this regime. Thus, the growth rate of the advective mode is always less than the feedback rate, and always increases as the feedback rate increases.

Figure 4 shows the growth rate of the advective mode as a function of zonal wavelength, for a feedback rate of 10^{-5} s^{-1} (chosen to be competitive with baroclinic instability), a meridional wavelength of 10,000 km, and a vertical wavelength of 10 km. Consistent with (3.25), the growth rate decreases with increasing zonal scale. For very short zonal scales, condition (3.24) applies, so that by (3.25) the growth rate is approximately equal to the feedback rate when the zonal scale is much less than the internal deformation radius, i.e., when $k_x^2 \gg f_0^2 n^2 / N^2$. For the 10 km vertical wavelength, the internal deformation radius is 1000 km.

Figure 5 shows the advective mode growth rate as a function of vertical wavelength, for a feedback rate of 10^{-5} s^{-1} and zonal and meridional wavelengths of 1000 km. For such a horizontal scale, the external Rossby wave frequency is 1.3×10^{-6} s^{-1}, much less than the assumed feedback rate, so that most waves will satisfy the condition (3.24). Consistent with the corresponding approximate solution (3.25), the growth rate increases as the vertical scale increases, eventually reaching the feedback rate for waves whose internal deformation radius is much larger than the horizontal scale of the wave.

In summary, the growth rate of the advective mode is always less than the radiative-dynamical feedback rate. It increases with increasing feedback rate, increasing vertical scale, and decreasing meridional and zonal scale. The latter scale dependence suggests the requirement that the basic state be horizontally uniform need only hold for spatial scales as small as the internal deformation radius. Although Figures 4 and 5 consider only feedback rates less than the Coriolis frequency,

(4.11) tells us that the same qualitative scale dependence of the advective mode growth rate also holds for feedback rates larger than the Coriolis frequency.

According to (4.10) and (4.11), the growth rate of the inertia-gravity modes for negative radiative-dynamical feedback (absorber increasing with altitude) has the same scale dependence as that of the unstable advective mode, but with half the amplitude for the same feedback rate magnitude. However, the analysis leading to (4.10) and (4.11) is based on an f-plane. On a β-plane, we find that the β term enhances the growth rate of the advective mode when the feedback rate is less than the Rossby wave frequency. It remains to be seen whether the inertia-gravity modes are also affected by the β term. Figure 6 shows the gravity wave growth rate, normalized by the feedback rate, as a function of the feedback rate, for zonal and meridional wavelengths of 1000 km and a vertical wavelength of 10 km. For feedback rates much larger than the Coriolis frequency (10^{-4} s^{-1}), (4.11) applies, with the growth rate increasing with the cube root of the feedback rate. For feedback rates much less than the Coriolis frequency, (4.10) applies, with the growth rate proportional to the feedback rate, even for feedback rates much less than the Rossby wave frequency. Thus, the analysis of the inertia-gravity mode on the f-plane is a good approximation for all feedback rates. Because the growth rates of the gravity and advective modes have the same scale dependence for feedback rates larger than the Rossby wave frequency, we need not discuss the scale dependence of the gravity modes, but refer the reader to the previous discussion of the advective mode.

Of the three modes of instability, the Rossby mode is the most complex in terms of its parametric dependence. The analysis of section 3 considered a wide range in the feedback rate, from values much smaller than the Rossby wave frequency to values much larger, but was restricted by the quasi-geostrophic approximation. However, consistent with the fact that Rossby waves are low-frequency modes, the

more general primitive equation solution of (4.13) for the Rossby mode is virtually identical to the quasi-geostrophic solution. Thus, the approximate solutions (3.22) and (3.25) for the Rossby mode are valid for feedback rates larger than the Coriolis frequency as well as smaller.

Figure 7 shows the growth rate of the Rossby mode as a function of the feedback rate, for a variety of zonal, meridional and vertical wavelengths. The most notable feature of Figure 7 is that for each wave scale the Rossby mode growth rate peaks at a specific feedback rate. This result is consistent with (3.22) and (3.25), which indicate that for small feedback rates the Rossby mode growth rate increases as the magnitude of the feedback rate increases, but for large feedback rates the growth rate decreases as the feedback rate increases. The precise transition cannot be determined analytically, but appears to be given by (3.26) i.e., near the lower bound of the feedback rate given in (3.24). For each of the wave scales of Figure 7, this value of the feedback rate is indicated on the figure. The agreement between this value and the actual feedback rate of maximum growth rate is evidently quite good.

The scale dependence of the Rossby mode growth rate also exhibits some interesting features. Figure 8 shows the Rossby mode growth rate as a function of vertical wavelength for two different cases. One curve is for synoptic scale waves with zonal and meridional wavelengths of 1000 km and a feedback rate of -10^{-5} s^{-1}, while the other curve is for planetary scale waves with zonal and meridional wavelengths of 10,000 km and a feedback rate of -10^{-4} s^{-1}. In both cases the growth rate is largest for an intermediate vertical wavelength. Although the parametric dependence is quite complex (for details the interested reader is refered to Ghan, 1988a), the rule of thumb, based on a wide variety of cases, seems to be that the growth rate for a given feedback rate and specified zonal and meridional

scales is largest for a vertical wavelength corresponding to an internal deformation radius somewhat smaller than each of the horizontal wavelengths.

The dependence of the Rossby mode growth rate on zonal scale is also complicated. In general, the growth rate for a given feedback rate and specified vertical and meridional scales is largest for zonal scales somewhat longer than the deformation radius. For example, Figure 9 shows the Rossby mode growth rate as a function of zonal wavelength for a meridional wavelength of 1000 km, a vertical wavelength of 10 km, and a feedback rate of -10^{-4} s^{-1}. The growth rate is seen to peak at a zonal wavelength of about 1500 km, somewhat longer than the deformation radius of about 1000 km. For more details concerning the dependence of the growth rate on zonal scale, see Ghan (1988a).

The dependence of the Rossby mode growth rate on the meridional scale is much simpler: for all parameter regimes, the growth rate increases as the meridional scale of the perturbation increases. Thus, waves with the largest meridional scale consistent with the horizontal domain of the radiative-dynamical feedback will grow fastest in the linear stage.

We have so far only considered the scale dependence of the growth rate for each dimension separately. A more general question is: for which three-dimensional wave vector is the Rossby mode growth rate largest? According to the analysis of section 3, the Rossby mode growth rate is much less than the feedback rate when condition (3.24) is satisified, but can be as large as the feedback rate when condition (3.20) is satisfied. When (3.20) is satisfied, the feedback rate is largest for waves that are shallow and long, i.e., $f^2n^2 \gg N^2k_2^2$. However, if the waves are too shallow, the internal Rossby wave frequency won't exceed the feedback rate, so that condition (3.20) is not satisfied. Thus, the growth rate is largest for waves that are very long and deep enough to satisfy (3.20). This is illustrated in Figure 10, which shows the Rossby mode growth rate contoured as a function of zonal and vertical wavelength

for a meridional wavelength of 10,000 km, and a feedback rate of -10^{-5} s^{-1}. The growth rate is seen to increase as the zonal and vertical scales are progressively increased.

For many problems the zone of strong radiative dynamical feedback may be somewhat restricted. For example, a layer of strong absorber gradient may span only a few kilometers. In that case the vertical wavelength of the unstable modes should not exceed the vertical span of strong feedback. The zonal scale of the fastest growing Rossby mode would then be limited somewhat.

The analysis of the primitive equations on a mid-latitude β-plane has so far been based on (4.12), which admits nontrivial solutions if the meridional velocity is nonzero. If, on the other hand, the meridional velocity is identically zero, the primitive equations can be reduced to a single wave equation for the vertical velocity,

$$D^3 \frac{\partial}{\partial z} \frac{1}{\rho_0} \frac{\partial}{\partial z} (\rho_0 w) - N^2 (D - \alpha) w_{xx} = 0 \quad . \tag{4.14}$$

Substituting solutions of the form (3.14) yields the algebraic relation

$$n^2 D^3 - N^2 (D - \alpha) k^2 = 0 \quad . \tag{4.15}$$

This cubic equation is identical to the corresponding equation for the primitive equations on an f-plane, except that the two-dimensional wavenumber k_2^2 has been replaced by the zonal wavenumber k^2, and the Coriolis parameter is absent. Thus, in the absence of radiative-dynamical feedback, it describes an advective mode and two gravity (rather than inertia-gravity) modes. The Rossby mode is missing because the meridional velocity is identically zero. In the presence of the radiative-dynamical feedback, the analysis of section 4.a applies, but with the two-dimensional and three-dimensional wavenumbers replaced by the zonal wavenumber. Thus, for positive radiative-dynamical feedback, the advective mode is unstable in the absence of dissipation and the gravity modes are damped, while

for negative feedback the advective mode is damped and the gravity modes are unstable. For weak radiative-dynamical feedback (i.e., $|\alpha| \ll Nk/n$), the growth rates are, in the absence of dissipation, proportional to the feedback rate, while for strong feedback ($|\alpha| \gg Nk/n$) the growth rate is proportional to the cube root of the feedback rate. The maximum growth rate of the advective mode is the feedback rate, which occurs for all wavenumbers such that $|\alpha| \ll Nk/n$. The maximum growth rate of the gravity modes is one half the feedback rate, which again occurs for all wavenumbers such that $|\alpha| \ll Nk/n$. In no instance does the advective mode propagate, while the frequency of the gravity modes dominates the growth rate except when $|\alpha| \gg Nk/n$.

Finally, consider the application of radiative-dynamical feedback to the tropical atmosphere, in which it is not reasonable to treat the Coriolis parameter as a constant in (4.12). Following the classical theory of equatorial β-planes, we approximate the Coriolis parameter as a linear function of latitude. Equation (4.12) then becomes

$$\left(D^2 - \beta^2 y^2\right) D^2 \frac{\partial}{\partial z} \frac{1}{\rho_0} \frac{\partial}{\partial z} (\rho_0 v) - N^2 (D - \alpha) \left(D\nabla^2 - \beta \frac{\partial}{\partial x} \right) v = 0 \quad . \quad (4.16)$$

Because the coefficients of (4.16) are no longer constant, the simple plane-wave solution form (3.14) is inappropriate. Following the classical theory, we express solutions in the form

$$v = V(y) \exp[z/2H] \exp[i(kx - mz - \sigma t)] \quad (4.17)$$

which reduces (4.18) to the ordinary differential equation

$$N^2 (D - \alpha) D V_{yy} - \beta^2 y^2 D^2 n^2 V - \left[N^2 (D - \alpha)(\beta i k - k^2 D) - D^4 n^2 \right] V = 0 \ . \quad (4.18)$$

To reduce (4.18) to canonical form, we introduce the scaling $y = r\varphi$ and choose

$$r^4 = \frac{N^2 (D - \alpha) D}{\beta^2 D^2 n^2} \quad (4.19)$$

Then (4.18) reduces to

$$V_{\phi\phi} - \phi^2 V + \left[\frac{N^2 (D - \alpha) \left(\beta i k - k^2 D \right) - D^4 n^2}{r^2 \beta^2 D^2 n^2} \right] V = 0 \quad . \tag{4.20}$$

We can now expand solutions in a series of Hermite functions,

$$V(\phi) = \sum_{\ell} \bigvee_{\ell} H_{\ell}(\phi) \tag{4.21}$$

and apply the orthogonality relation

$$H_{\ell}'' - \phi^2 H_{\ell} = -(2\ell - 1) H_{\ell} \tag{4.22}$$

to reduce (4.20) to the algebraic equation

$$n^2 D^4 - N^2 (D - \alpha) \left(k^2 D - i k \beta \right) + (2\ell - 1) N \beta n D \sqrt{D(D - \alpha)} = 0 \quad . \tag{4.23}$$

Equation (4.23) has eight solutions for D. However, because D determines the meridional scaling (4.19), some of these solutions cannot satisfy the lateral boundary conditions of boundedness. To see this, consider solutions with zero meridional velocity. Then the β term vanishes and the dispersion relation (4.23) reduces to

$$n^2 D^3 - N^2 (D - \alpha) k^2 = 0 \quad . \tag{4.24}$$

Equation (4.24) is very similar to (4.7) without the Coriolis term. The analysis of section 4.a demonstrates that two of the three solutions correspond to eastward and westward propagating gravity waves, and the third represents the advective mode, which does not propagate at all. From the momentum equations with $v = 0$ we find that

$$\Phi = \Phi_0 \exp \left(-\frac{1}{2} y^2 \frac{k\beta}{iD} \right) \exp[i(kx - mz - \sigma t)] \quad . \tag{4.25}$$

In order to satisfy the boundedness condition for large y, the imaginary part of D cannot be positive. Thus, only the eastward propagating (Kelvin) mode and

the advective mode satisfy the boundary conditions: the westward propagating solution must be rejected. In contrast with the classical theory, in which D is purely imaginary and hence the solution is a Gaussian, D is complex in the presence of feedback, and solutions oscillate in latitude.

Because of the large number of solutions of (4.23), we shall not attempt further investigation of the equatorial β-plane here. Given the ubiquity of unstable modes in midlatitudes for nonzero meridional velocity and in the tropics for zero meridional velocity, we would expect to find additional unstable solutions of (4.23).

5. Uniform Feedback: Absorber Distributions for Semi-Infinite Atmospheres

In the development of this basic theory of radiative-dynamical interactions, we have adopted the assumption that the radiative-dynamical feedback rate is uniformily distributed throughout the atmosphere. It is not obvious that such an assumption is reasonable for a semi-infinite atmosphere. If the radiative-dynamical feedback rate is constrained to be constant, one might expect that at some high altitude the basic state absorber concentration implied by such a constraint must become negative (for positive feedback) or unrealistically large (for negative feedback). If the resulting absorber distributions are unrealistic, we have a strong incentive to consider the more general problem of nonuniform feedback. Here we shall consider the question of what absorber distributions yield feedback rates that are uniform. We shall find that certain plausible absorber distributions are consistent with uniform radiative-dynamical feedback throughout a semi-infinite atmosphere.

Assuming that the density scale height and Brünt-Vaisala frequency are also constant, the feedback rate

$$\alpha = -\frac{RS_0 a}{c_p N^2 H}\,\bar{T}\,\frac{d\bar{q}}{dz} \tag{5.1}$$

is constant if

$$\frac{d^2\bar{q}}{dz^2} + \frac{a\rho_0}{\mu}\,\bar{q}\,\frac{d\bar{q}}{dz} = 0 \quad . \tag{5.2}$$

To determine analytical expressions for the absorber distribution that satisfy (5.2), we shall assume that both the specific absorption a and the density ρ_0 are constant. Defining the non-dimensional measure of altitude, $\zeta = a\rho_0 z/\mu$, (5.2) becomes

$$\bar{q}'' = -\frac{1}{2}\left(\bar{q}^2\right)' \tag{5.3}$$

or, upon integration,

$$\bar{q}' = -\frac{1}{2}\,\bar{q}^2 - C \quad . \tag{5.4}$$

where C is the integration constant.

There are several possible solutions to (5.4). If $C = -2C_1^2$, then one solution of (5.4) is

$$\bar{q}(\zeta) = 2C_1 \tan(C_2 - C_1\,\zeta) \quad . \tag{5.5}$$

From (5.4) one finds that the absorber mixing ratio decreases with altitude for this case. However, (5.5) can only apply to finite atmospheres, in which the argument of the tangent varies by less than π. A second solution of (5.4) for $C = -2C_1^2$ is

$$\bar{q}(\zeta) = 2C_1 \cot(C_1\zeta - C_2) \tag{5.6}$$

which is identical to (5.5) shifted by $\pi/2$.

If $C = 2C_1^2$, then two other solutions to (5.4) are

$$\bar{q}(\zeta) = 2C_1 \coth(C_1\,\zeta + C_2) \tag{5.7}$$

and

$$\bar{q}(\zeta) = 2C_1 \tanh(C_1\,\zeta - C_2) \quad . \tag{5.8}$$

Whereas (5.7) yields absorber distributions that also decrease with height, (5.8) applies to absorbers increasing with height. Both (5.7) and (5.8) yield positive absorber concentrations for semi-infinite as well as finite atmospheres, and hence ought to prove more useful in representing the distribution of absorber mixing ratio. However, a semi-infinite atmosphere requires a realistic representation of density. Because we have assumed density to be constant in solving (5.2), our solutions are only formally valid for relatively shallow atmospheres. We shall now, therefore, consider numerical solutions of (5.2) for density decreasing exponentially with scale height H.

Figure 11 shows four vertical distributions of absorber mixing ratio determined from the numerical solution of (5.2), subject to the boundary conditions $\bar{q}(0) = 0$ and $\bar{q}_z(0) = 5 \times 10^{-12}$, 1×10^{-11}, 2×10^{-11} and 5×10^{-11} m^{-1}. The resemblance between the curves and the hyperbolic tangent solution (5.8) is apparent, suggesting that variations in atmospheric density do not qualitatively alter the solutions. Note that because the hyperbolic tangent is bounded by unity, the solution (5.8) does not produce physically unreasonable distributions of absorber mixing ratio at high altitude.

The radiative-dynamical feedback rates (as defined by (5.1)) corresponding to the four absorber distributions illustrated in Figure 11 are -1.23×10^{-6}, -1.46×10^{-6}, -1.32×10^{-6}, and -6.81×10^{-7} s^{-1} for the surface gradients $\bar{q}_z(0) = 5 \times 10^{-12}$, 1×10^{-11}, 2×10^{-11} and 5×10^{-11} m^{-1}, respectively, assuming a specific absorption coefficient of 1000 $m^2 kg^{-1}$, a solar constant of 1360 W m^{-2}, a solar zenith angle of 60°, and a Brünt-Vaisala frequency of 10^{-2} s^{-1} (the specific choice for the value of the absorption coefficient, though appropriate for smoke, is arbitrary in that the feedback depends only on the product $a\bar{q}$; the same feedback rates would therefore arise for different absorption coefficients if the basic state absorber mixing ratio is scaled accordingly). The numerical integration of (5.2) was only carried to an altitude of 30 km. Above this level, the mixing ratio is assumed to be constant; given the reduced atmospheric density at altitude, the error incurred by such a treatment is small because for weak surface gradients in the absorber mixing ratio there is little attenuation of the solar beam, while for strong surface gradients the distribution rapidly approaches the asymptotic limit of the hyperbolic tangent and hence is consistent with the treatment of uniform mixing ratio above the model top. Note that the feedback rate is greatest for the intermediate surface absorber gradient, in which the absorption optical depth from the top of the atmosphere to the surface is roughly equal to the cosine of the solar zenith angle. For larger

surface gradients the transmission of sunlight to the surface is reduced to very low levels, while for smaller surface gradients the transmission is nearly complete but, because the surface gradient is low, the feedback rate is also small.

According to the analysis for constant density, several solutions that preserve a constant feedback rate are possible when the absorber distribution decreases with altitude. Figure 12 shows two vertical distributions of absorber mixing ratio determined from numerical solutions of (5.2), subject to the boundary conditions $\bar{q}(0) = 10^{-6}$ and $\bar{q}_z(0) = -8 \times 10^{-10}$ m^{-1} and $\bar{q}_z(0) = -9 \times 10^{-10}$ m^{-1}. Although the boundary conditions for these two solutions are very similar, the distribution of absorber concentration at high altitudes is qualitatively very different. When the surface gradient is weak, the mixing ratio approaches an asymptotic limit at high altitude, a characteristic in common with the hyperbolic cotangent in the analytical solution (5.7). When the surface gradient is sufficiently strong, however, the absorber mixing ratio becomes negative at high altitudes. This is a feature of the cotangent function in solution (5.6).

The radiative-dynamical feedback rates for these two solutions are also quite different. For the solution with the weaker surface gradient, the feedback rate is 4×10^{-8} s^{-1}, while for the stronger surface gradient the feedback rate is 4×10^{-6} s^{-1} (except at those altitudes at which the absorber mixing ratio is zero). These feedback rates differ so much, even at the surface where the surface gradients are similar, because the transmissivity of the weak feedback solution is reduced by absorption at higher altitudes.

6. Summary

The theory developed here demonstrates the potential for unstable radiative-dynamical interactions that are strong enough to compete with other purely dynamical instability mechanisms. Two distinct modes have been identified, described as advective and propagating modes, respectively.

In the advective mode, an instability typically arises when the absorber mixing ratio decreases with altitude. Perturbations in absorber concentration, shortwave radiative heating, vertical motion and temperature are all in phase. Propagation with respect to the mean flow is weak. Amplification is most rapid for modes that are short and deep, i.e., for modes with horizontal scales much less than the internal deformation radius. Thus, the requirement that the basic state be horizontally uniform is satisfied for absorber distributions varying on spatial scales larger than the deformation radius, and hence may hold in a variety of geophysical applications.

Propagating modes such as Rossby and inertia-gravity waves become unstable when the absorber mixing ratio increases with altitude. High absorber concentrations and strong heating lag downward motion by about one quarter cycle; warm temperatures lag the heating by one quarter cycle, and hence are in phase with upward motion. Because strong propagation is necessary to maintain the proper phase relationships for energy release, the growth rate of propagating modes is typically much less than the frequency of oscillation. This constraint limits the growth rate of the slowly propagating Rossby waves. The scale dependence of the growth rate of the Rossby and inertia-gravity modes is quite different, with growth of the Rossby modes most rapid for waves slightly longer than the internal deformation radius, and growth of inertia-gravity modes most rapid for waves much shorter than the deformation radius. Thus, while the assumption that the basic state is

horizontally uniform will rarely hold for the Rossby mode, it will often apply in the case of the inertia-gravity modes.

The fundamental parameter that emerges from the analysis is the rate of radiative-dynamical feedback, defined as

$$\alpha \equiv -\frac{RS_0 a\bar{T}}{c_p N^2 H}\frac{\partial \bar{q}}{\partial z} \tag{6.1}$$

The growth rate of unstable disturbances has been found in most instances to be bounded by the magnitude of the feedback rate, so that α characterizes the growth rate. For basic state absorber distributions that decay exponentially with height, the feedback rate is largest at altitudes where the absorption optical depth equals the cosine of the solar zenith angle. In such cases, the maximum feedback rate, and hence the maximum growth rate, can be competitive with growth rates associated with baroclinic instability.

Several plausible absorber distributions consistent with uniform radiative-dynamical feedback have also been determined. These solutions are valid for semi-infinite atmospheres, and lend support to the assumption of uniform feedback rate adopted in the basic theory.

The extension of this basic theory to account for a number of complicating factors, including the effects of perturbations in transmissivity (associated with absorber perturbations at higher altitudes), dissipative processes, basic state vertical shear, and scattering, is discussed in the companion paper Ghan (1988b). In addition, the application of the theory to Martian dust storms is considered in Ghan and Covey (1988).

Acknowledgements

This paper is based on the author's PhD dissertation at MIT. The comments of my thesis advisor, Professor Peter Stone, as well as those by Professors Emanuel, Lindzen, and Lorenz and Dr. Rosen of my thesis committee led to significant generalizations of the theory. Discussions with my colleagues at Livermore, especially Karl Taylor, Curt Covey and Mike MacCracken, were also fruitful. Nancy Kliment and Floy Worden typed the manuscript. This work was performed under the auspices of the U.S. Department of Energy by the Lawrence Livermore National Laboratory under Contract No. W-7405-Eng-48.

APPENDIX A. Notation

t	time
x	zonal distance
y	meridional distance
z	vertical distance
p	pressure
u	zonal velocity
v	meridional velocity
w	vertical velocity
ζ	vorticity, $\frac{\partial v}{\partial x} - \frac{\partial u}{\partial y}$
ψ	horizontal streamfunction
Φ	geopotential
θ	potential temperature
q	absorber mixing ratio
ρ_0	atmospheric density
H	density scale height
c_p	specific heat at constant pressure
R	gas constant
κ	thermodynamic ratio R/c_p
N	Brünt-Vaisala frequency
μ	cosine of solar zenith angle
S_0	solar constant
a	specific absorption coefficient
Q	radiative heating rate
T	transmissivity from top of atmosphere
f	Coriolis parameter

β	meridional gradient of f
k	zonal wavenumber
ℓ	meridional wavenumber
m	vertical wavenumber
n	vertical wavenumber, $n^2 = m^2 + \left(4H^2\right)^{-1}$
k_2^2	$k^2 + \ell^2$
k_3^2	$k_2^2 + f^2 n^2 / N^2$
α	radiative-dynamical feedback rate
σ	wave frequency (complex)
D	advective operator
ϵ	dissipation rate
$\overline{(\ )}$	basic state
$(\ )'$	small perturbation from basic state

References

Ghan, S. J., 1988: *Unstable Radiative-Dynamical Interactions.* Ph.D. thesis, Massachusetts Institute of Technology.

Ghan, S. J., 1988: Unstable radiative-dynamical interactions. Part II: Expanded theory. *J. Atmos. Sci.*, submitted.

Ghan, S. J., and C. Covey, 1988: Unstable radiative-dynamical interactions. Part III: Application to Martia dust storms. *J. Atmos. Sci.*, to be submitted.

Gierasch, P. J., and R. M. Goody, 1973: A model of a Martian Great Dust Storm. *J. Atmos. Sci.*, *30*, 169–179.

Gierasch, P. J., A. P. Ingersoll, and R. T. Williams, 1973: Radiative instability of a cloud planetary atmosphere. *Icarus*, *19*, 473–481.

Haberle, R. M., C. B. Leovy, and J. B. Pollack, 1982: Some effects of global dust storms on the atmospheric circulation of Mars. *Icarus*, *50*, 322–367.

Haberle, R. M., T. P. Ackerman, O. B. Toon, and J. L. Hollingsworth, 1985: Global transport of atmospheric smoke following a major nuclear exchange. *Geophys. Res. Lett.*, *12*, 405–408.

Harshvardhan, R. Davies, D. A. Randall and T. G. Corsetti, 1987: A fast radiation parameterization for atmospheric circulation models. *J. Geophys. Res.*, *92*, 1009-10016.

Houben, H., 1981: A global Martian dust storm model. Presented at Third International Colloquium on Mars, Pasadena.

Leovy, C. B., 1966: Photochemical destabilization of gravity waves near the mesopause. *J. Atmos. Sci.*, *23*, 223–232.

Leovy, C. B., R. W. Zurek, and J. B. Pollack, 1973: Mechanisms for Mars dust storms. *J. Atmos. Sci.*, *30*, 749–762.

Leovy, C. B., and R. W. Zurek, 1979: Thermal tides and Martian dust storms: Direct evidence for coupling. *J. Geophys. Res.*, *84*, 2956–2968.

Lindzen, R. S., 1966: Radiative and photochemical processes in mesospheric dynamics: Part II, Vertical propagation of long period disturbances at the equator. *J. Atmos. Sci.*, *23*, 334–343.

Lindzen, R. S., 1966: Radiative and photochemical processes in mesospheric dynamics: Part III, Stability of a zonal vortex at mid-latitudes to axially symmetric disturbances. *J. Atmos. Sci.*, *23*, 344–349.

Lindzen, R. S., 1967: Planetary waves on beta planes. *Mon. Wea. Rev.*, *95*, 441-451.

Malone, R. C., L. H. Auer, G. A. Glatzmaier, M. C. Wood, and O. B. Toon, 1986: Nuclear winter: Three-dimensional simulations including interactive transport, scavenging, and solar heating of smoke. *J. Geophys. Res.*, *91*, 1039–1054.

Schneider, E. K., 1983: Martian great dust storms: Interpretive axially symmetric models. *Icarus*, *55*, 302–331.

Smagorinski, J., 1963: General circulation experiments with the primitive equations. I. The basic experiment. *Mon. Wea. Rev.*, *91*, 99-164.

Westphal, D. L., O. B. Toon, and T. N. Carlson, 1987: A two-dimensional numerical investigation of the dynamics and microphysics of Saharan dust storms. *J. Geophys. Res.*, *92*, 3027-3049.

Wiscombe, W. J., 1977: The delta-Eddington approximation for a vertically inhomogeneous atmosphere. NCAR Tech. Note 121 + STR.

Table 1. Approximate solutions for the complex eigenfrequency σ.

Mode	Feedback Rate				
	$\alpha \ll \frac{\beta k}{k_3^2}$	$\ll \lvert\alpha\rvert \ll$	$\frac{\beta k}{k_2^2}\frac{k_3^2}{k_2^2} \ll \alpha \ll$	$\frac{2Nk_2^2}{\sqrt{3}n\ k_3^2}$	$\ll \lvert\alpha$
Advective	$\frac{\alpha^2 k_3^2}{\beta k}\frac{f^2 n^2}{N^2 k_3^2} + i\alpha$	$(1-i)\alpha\left(\frac{\beta k}{2\alpha k_3^2}\right)^{1/2}$	$\frac{\beta k}{k_3^2}\frac{f^2 n^2}{N^2 k_3^2} + \frac{i\alpha k_2^2}{k_3^2}$		$i\alpha\left(\frac{N^2 k_2^2}{\alpha^2 n^2}\right)^{1/3}$
Rossby	$-\frac{\beta k}{k_3^2} - \frac{i\alpha f^2 n^2}{N^2 k_3^2}$	$-(1+i)\alpha\left(\frac{\beta k}{2\alpha k_3^2}\right)^{1/2}$	$-\frac{\beta k}{k_2^2} - \frac{i\beta^2 k^2}{\alpha}\frac{f^2 n^2}{N^2 k_2^6}$		
Gravity			$\pm\frac{Nk_3}{n} - \frac{i\alpha k_2^2}{2k_3^2}$	$-\alpha\left(\frac{i\pm\sqrt{3}}{2}\right)\left(\frac{N^2 k_2^2}{\alpha^2 n^2}\right)^{1/3}$	

Figure Captions

Figure 1. Absorber mixing ratio (mg/kg) simulated 30 days following an absorber initialization with a Gaussian horizontal distribution (standard deviation 3000 km) and a Gaussian vertical distribution with a maximum absorber mixing ratio of 10^{-6} at 10 km and a standard deviation of 5 km. The model is a two-dimensional slab-symmetric primitive-equation model on a midlatitude f-plane. Moist processes are not represented explicitly, but are rather treated by prescribing a horizontally uniform absolute humidity for the purposes of radiative heating, and adjusting the temperature lapse rate to that of a moist adiabat under supercritical conditions. Longwave radiative cooling is treated using the Harshvardhan et al. (1987) broad-band parameterization. Solar heating is simulated with the Wiscombe (1977) delta-Eddington model. Radiative constituents are water vapor, carbon dioxide, and ozone for the longwave, and ozone and the nominal absorber for the short wave. The solar zenith angle is 60°, the solar constant 680 W m^{-2}, and the specific absorption of the absorber is 10^3 m^2 kg^{-1}. The surface temperature is prescribed as for an ocean-covered planet, with simple drag laws for the exchange of heat and momentum at the surface. Sub-grid scale horizontal mixing is represented by a Smagorinsky (1963) type parameterization. The model domain is 10,000 km, with a horizontal grid spacing of 33 km as indicated by the axis tic marks. Details of the numerical model are given in Ghan (1988a).

Figure 2. Schematic structure of advective mode (top) and propagating mode (bottom) of radiative-dynamical instability. In the propagating mode, phase propagation is from left to right.

Figure 3. Advective mode growth rate normalized by the radiative-dynamical feedback rate, as a function of the feedback rate. Midlatitude beta-plane. The zonal and meridional wavelengths are 1000 km; the vertical wavelength is 10 km. The

Brünt-Vaisala frequency is 10^{-2} s^{-1}; the density scale height is 8 km. The Coriolis and internal Rossby wave frequencies are indicated.

Figure 4. Advective mode growth rate as a function of zonal wavelength, for a radiative-dynamical feedback rate of 10^{-5} s^{-1} and a meridional wavelength of 10,000 km. Otherwise as in Figure 3. The internal deformation radius is indicated.

Figure 5. Advective mode growth rate as a function of vertical wavelength, for a radiative-dynamical feedback rate of 10^{-5} s^{-1}. Otherwise as in Figure 3.

Figure 6. Normalized inertia-gravity mode growth rate as a function of the radiative-dynamical feedback rate. Otherwise as in Figure 3.

Figure 7. Rossby mode growth rate as a function of the radiative-dynamical feedback rate for zonal and meridional wavelengths of 1000 km and a vertical wavelength of 10 km (solid line); for a zonal wavelength of 1000 km, a meridional wavelength of 10,000 km, and a vertical wavelength of 10 km (long dashed line); for zonal and meridional wavelengths of 1000 km and a vertical wavelength of 1 km (medium dashed line); and for a zonal wavelength of 10,000 km, a meridional wavelength of 1000 km, and a vertical wavelength of 10 km (short dashed line). Otherwise as in Figure 3.

Figure 8. Rossby mode growth rate as a function of vertical wavelength for zonal and meridional wavelengths of 1000 km and a radiative-dynamical feedback rate of -10^{-7} s^{-1} (solid line); and for zonal and meridional wavelengths of 10,000 km and a feedback rate of -10^{-6} s^{-1} (dashed line). Otherwise as in Figure 3.

Figure 9. Rossby mode growth rate as a function of zonal wavelength for a meridional wavelength of 1000 km, a vertical wavelength of 10 km, and a radiative-dynamical feedback rate of -10^{-4} s^{-1}. Otherwise as in Figure 3.

Figure 10. Rossby mode growth rate as a function of zonal and vertical wavelengths, for a radiative-dynamical feedback rate of -10^{-5} s^{-1}. Otherwise as in Figure 3.

Figure 11. Vertical distribution of basic state absorber mixing ratio that yields a uniform radiative-dynamical feedback rate, for a zero surface mixing ratio and vertical gradients at the surface of 5×10^{-12} m^{-1} (solid line), 1×10^{-11} m^{-1} (short dashed line), 2×10^{-11} m^{-1} (medium dashed line), and 5×10^{-11} m^{-1} (long dashed line). The specific absorption coefficient is assumed to be 1000 m^2 kg^{-1}, the solar zenith angle 60°, and the density scale height 8 km.

Figure 12. Vertical distribution of basic state absorber mixing ratio that yields a uniform radiative-dynamical feedback rate, for a surface mixing ratio of 10^{-6} and vertical gradients at the surface of -9×10^{-10} m^{-1} (solid line) and -8×10^{-10} m^{-1} (dashed line). Otherwise as in Figure 11.

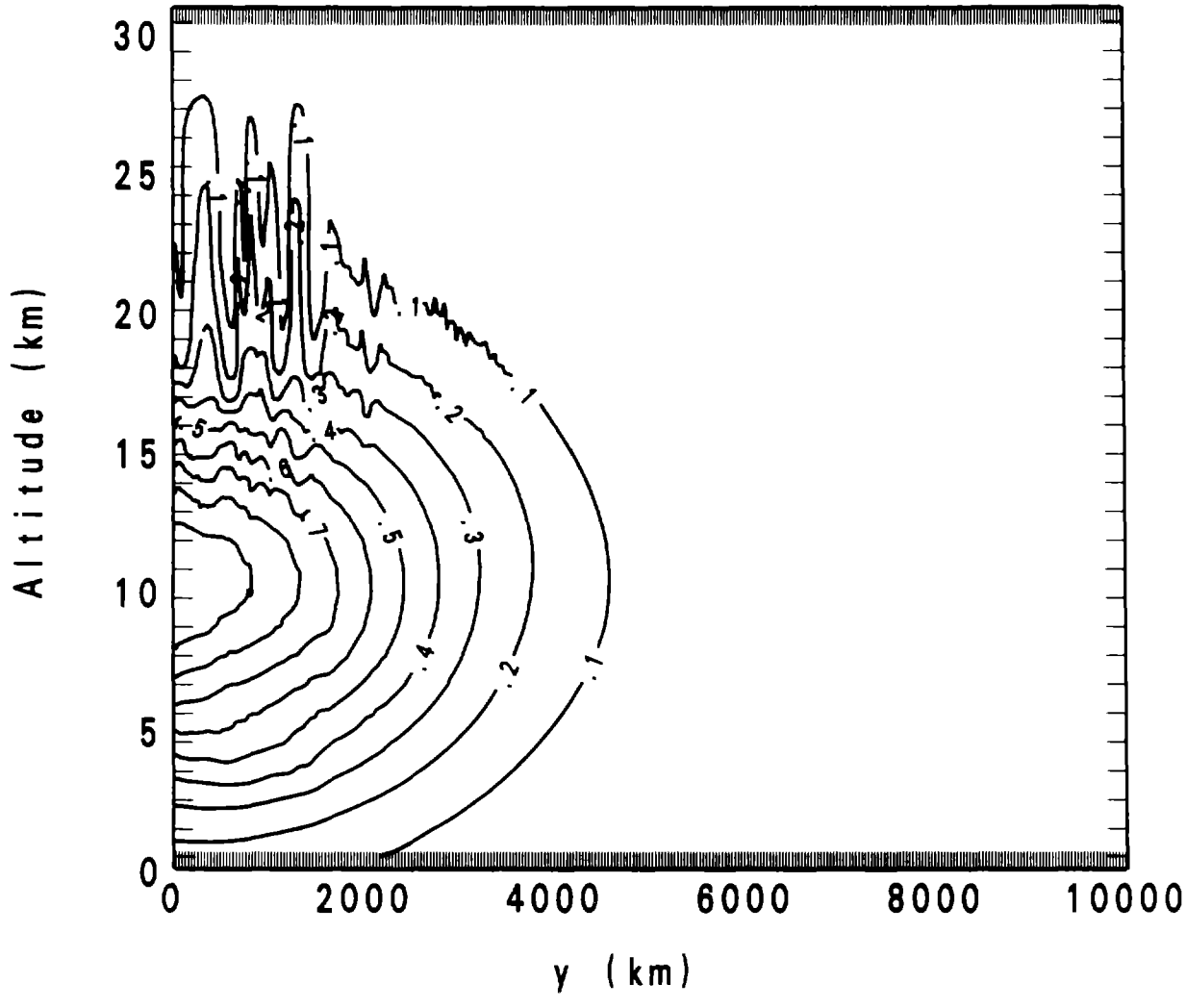

F.g. 1

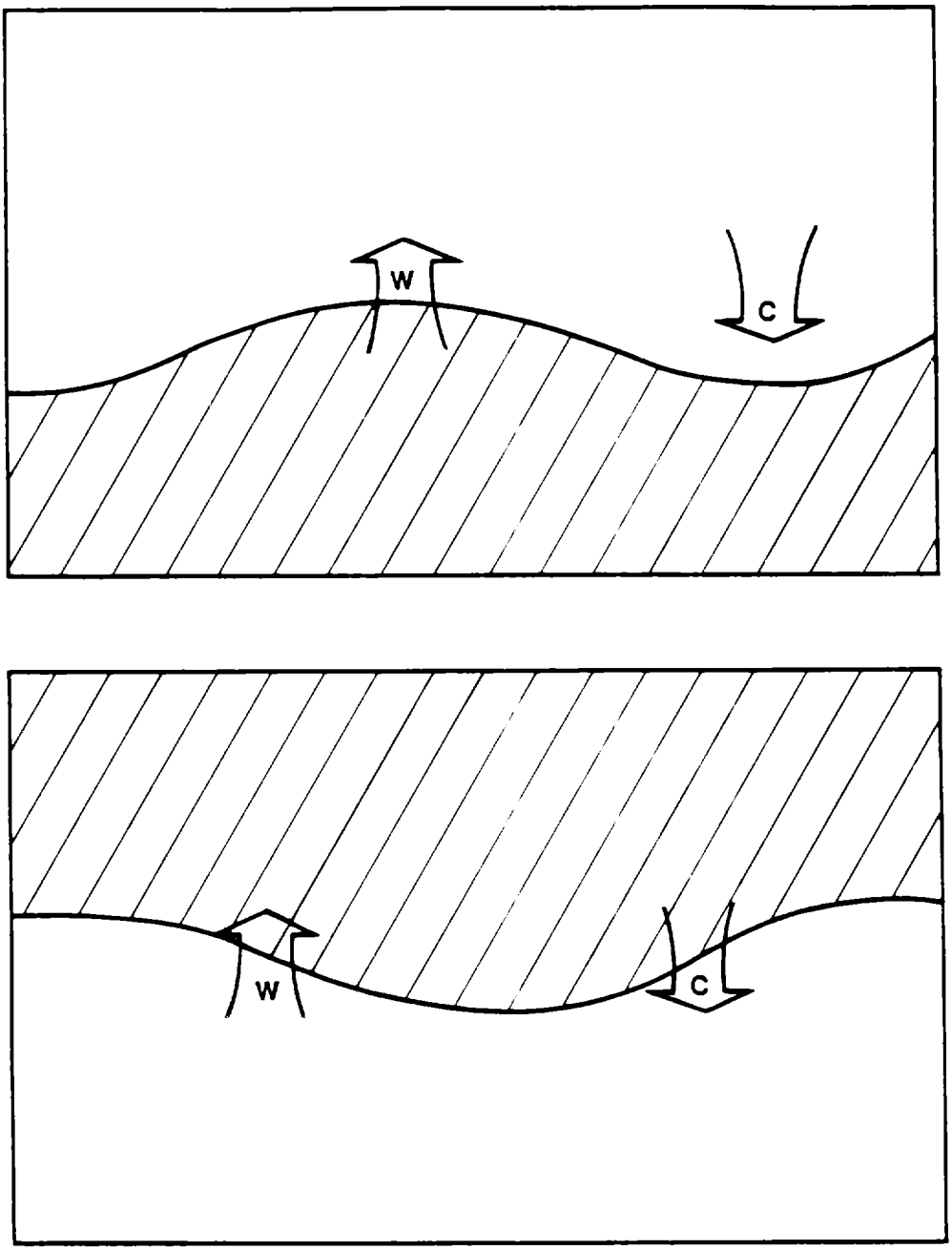

Fig. 2

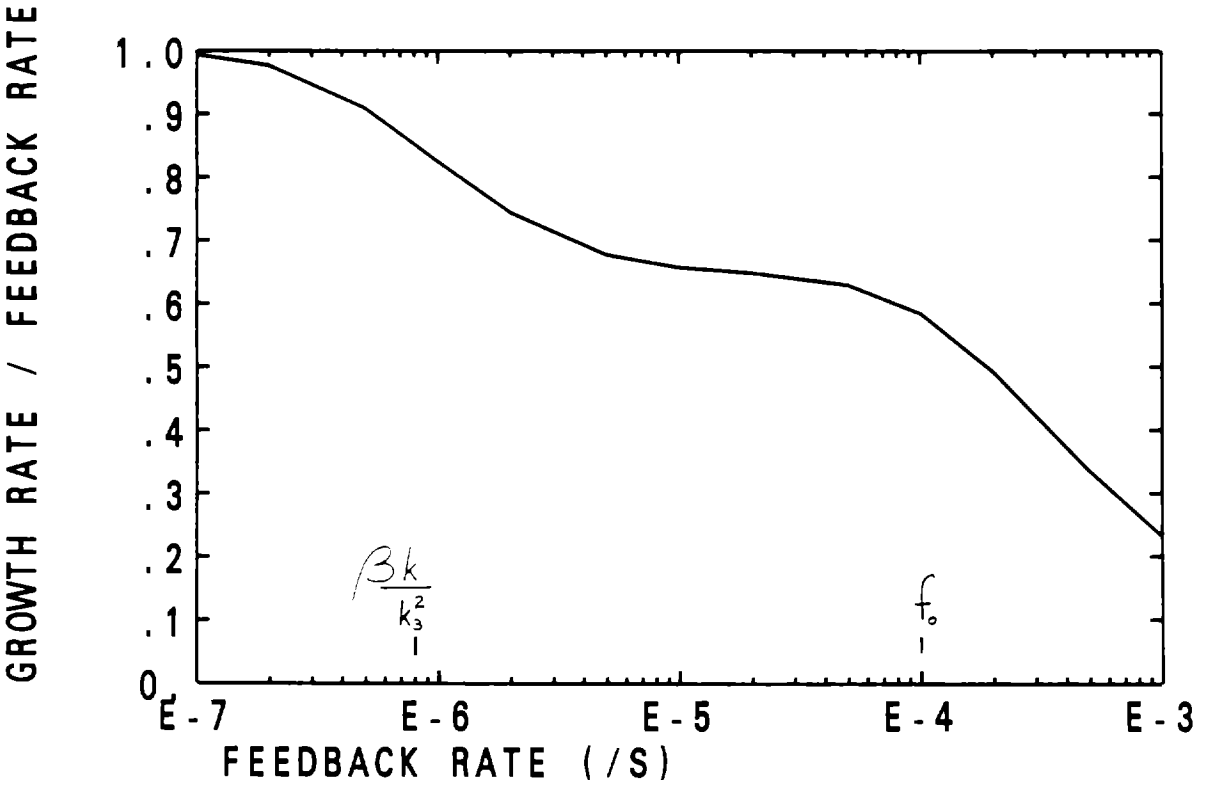
GROWTH RATE / FEEDBACK RATE
1.0
.9
.8
.7
.6
.5
.4
.3
.2
.1
0
E-7
E-6
E-5
E-4
E-3
FEEDBACK RATE (/S)
βk / k₃²
f₀

Fig. 3

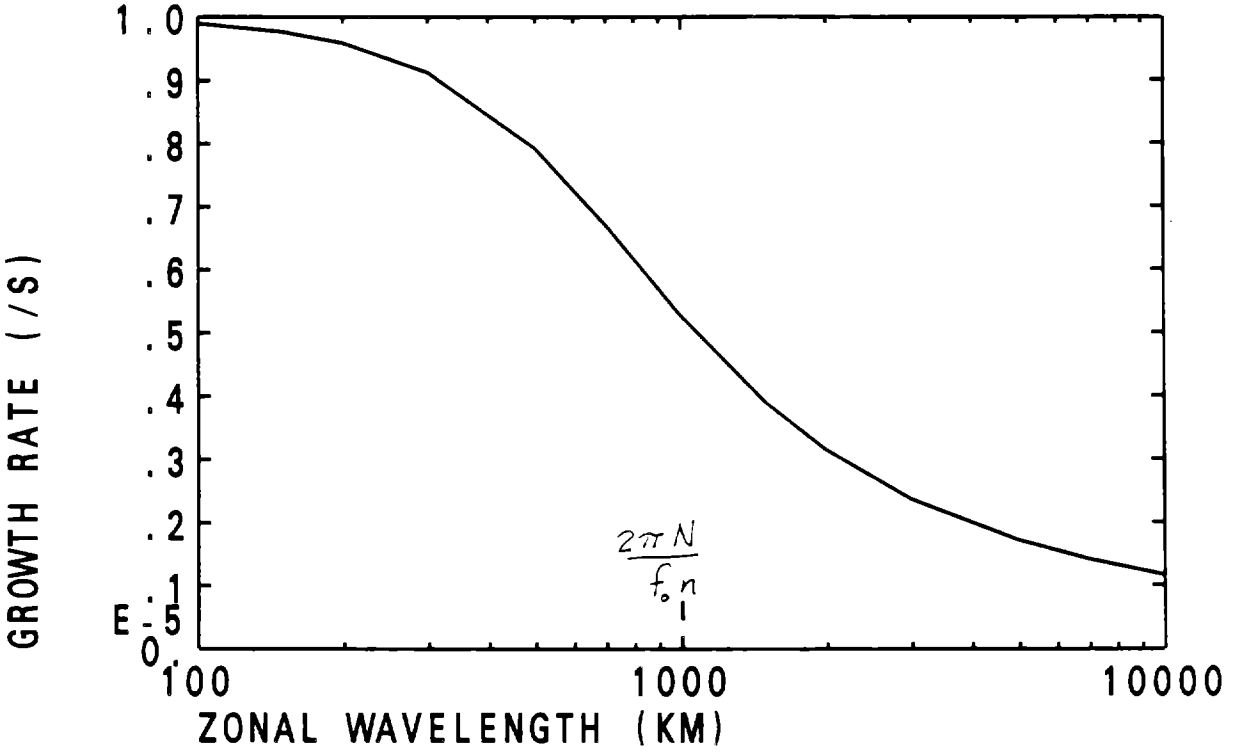
GROWTH RATE (/S)
1.0
.9
.8
.7
.6
.5
.4
.3
.2
.1
E-5
0
100
1000
10000
ZONAL WAVELENGTH (KM)
2πN/f₀n
1

Fig. 4

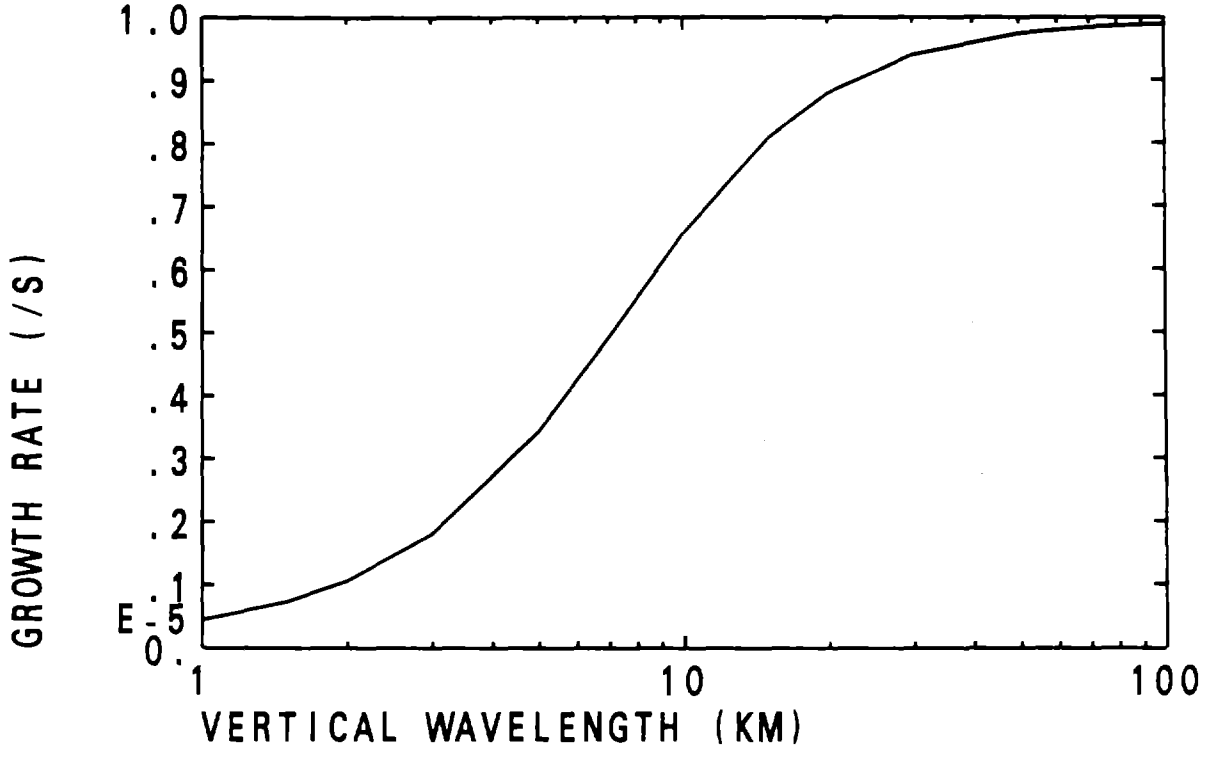
GROWTH RATE (/S)
1.0
.9
.8
.7
.6
.5
.4
.3
.2
.1
E-5
0.
1
10
100
VERTICAL WAVELENGTH (KM)

Fig. 5

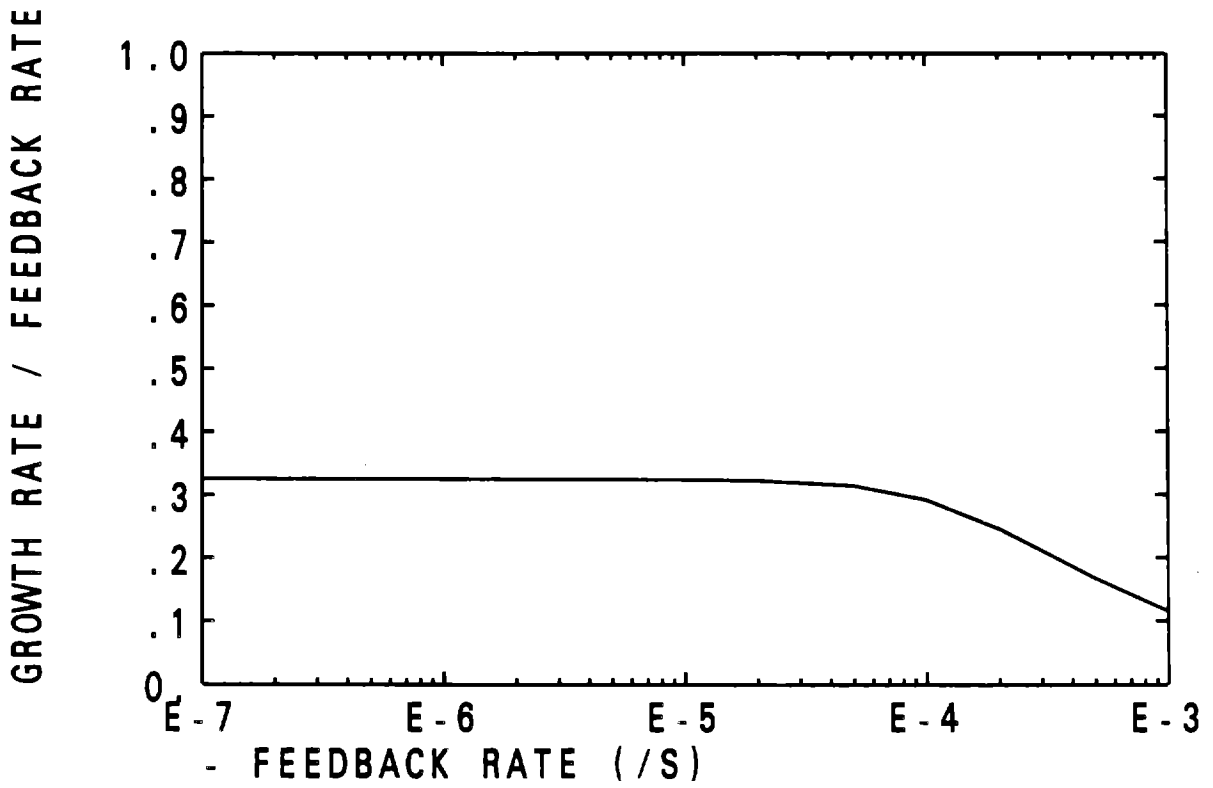
GROWTH RATE / FEEDBACK RATE
1.0
.9
.8
.7
.6
.5
.4
.3
.2
.1
0
E-7
E-6
E-5
E-4
E-3
- FEEDBACK RATE (/S)

Fig. 6

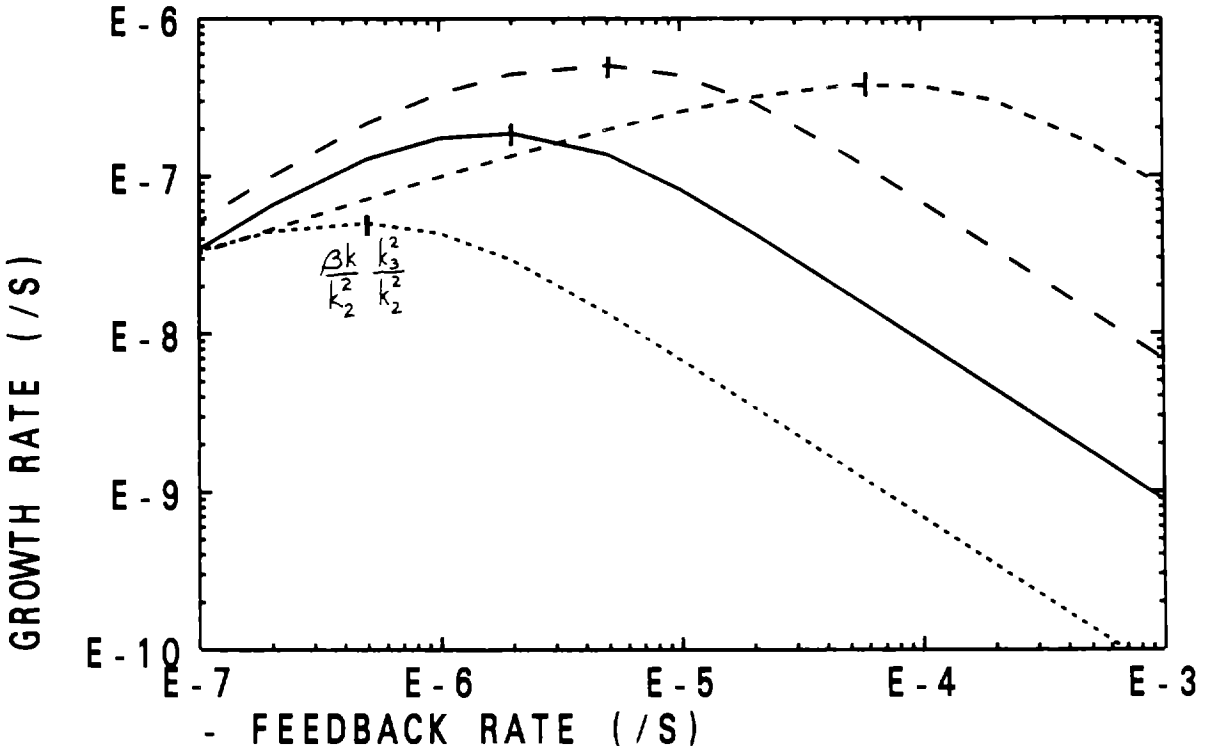
E-6
E-7
E-8
E-9
E-10
GROWTH RATE (/S)
$\frac{\beta k}{k_2^2}\frac{k_3^2}{k_2^2}$
E-7
E-6
E-5
E-4
E-3
- FEEDBACK RATE (/S)

Fig 7

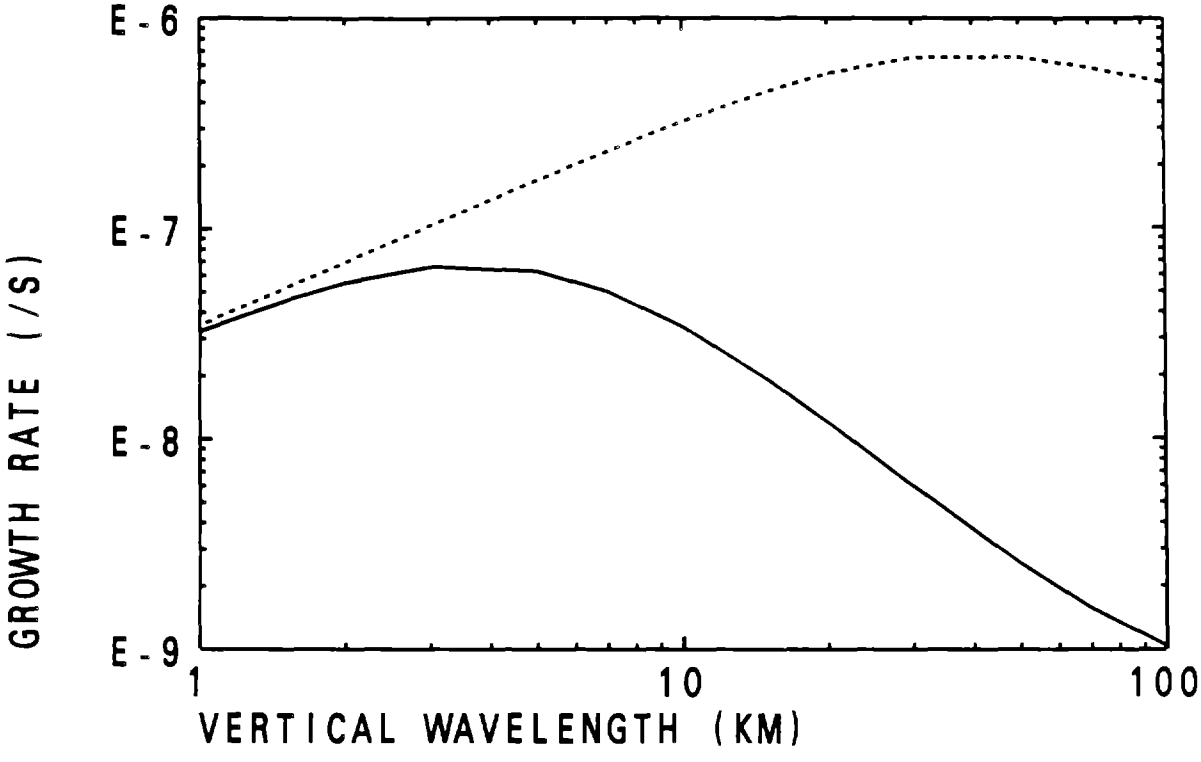

Fig. 8

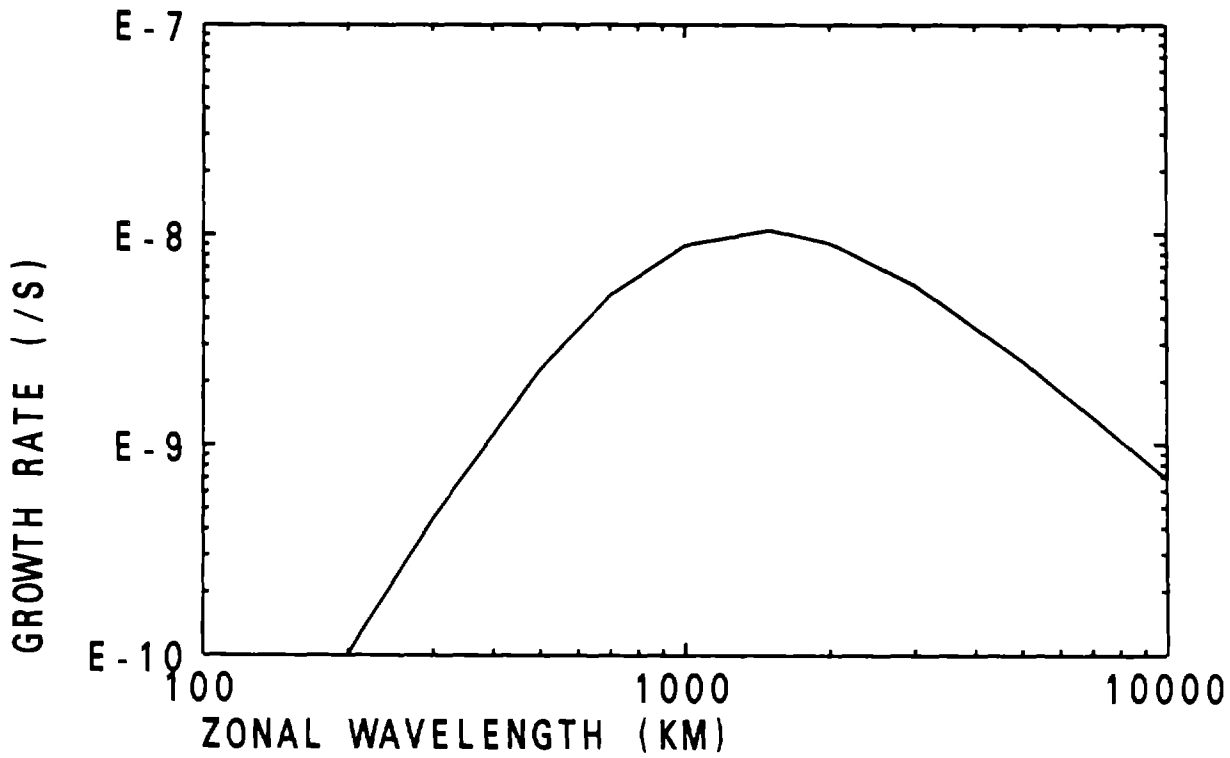

Fig 9

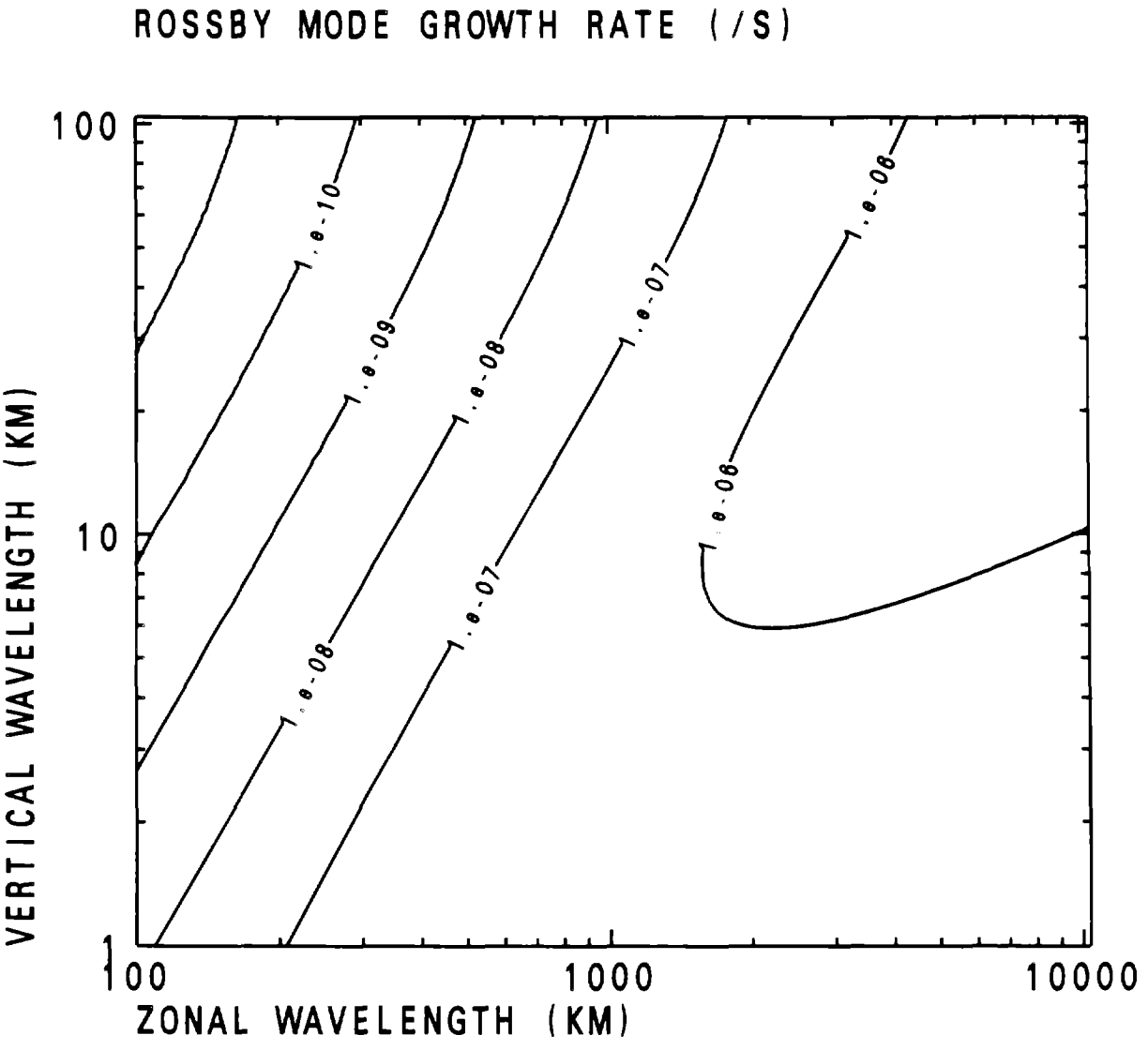
ROSSBY MODE GROWTH RATE (/S)
100
10
1
VERTICAL WAVELENGTH (KM)
100
1000
10000
ZONAL WAVELENGTH (KM)
1.e-10
1.e-09
1.e-08
1.e-08
1.e-07
1.e-07
1.e-08
1.e-06

Fig 10

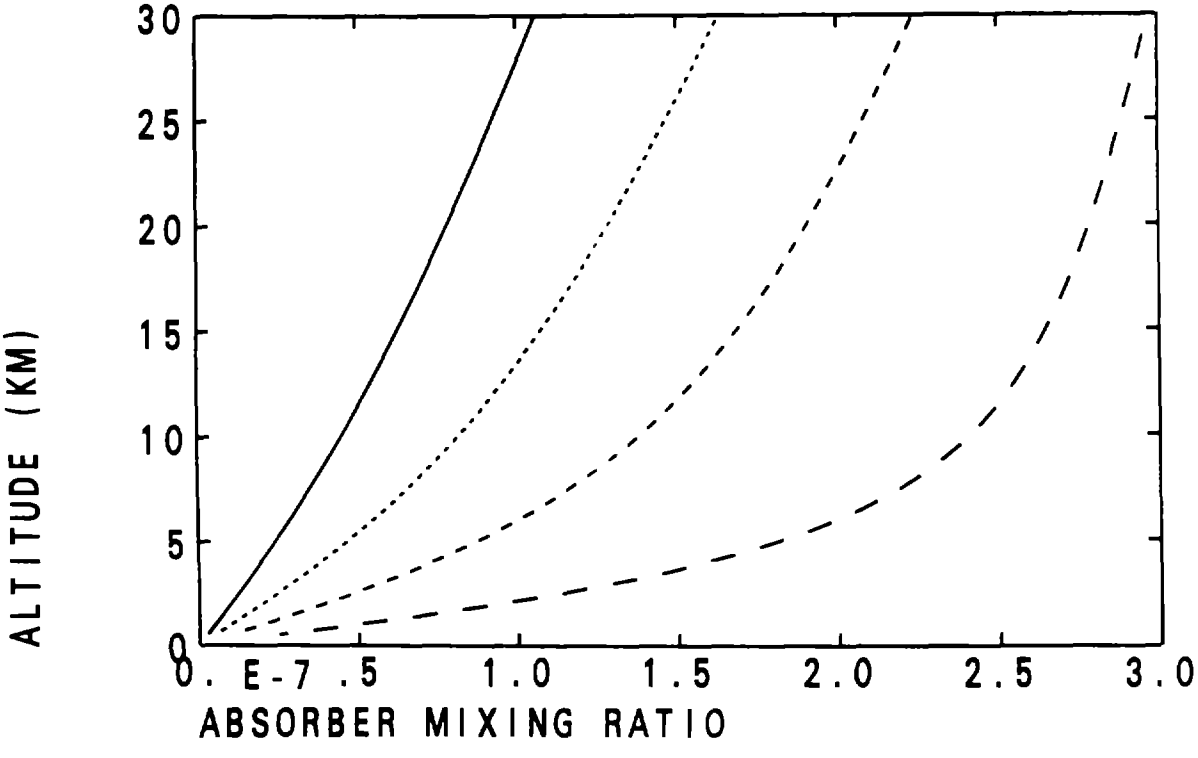
30
25
20
15
10
5
0
ALTITUDE (KM)
0. E-7 .5
1.0
1.5
2.0
2.5
3.0
ABSORBER MIXING RATIO

Fig. 11

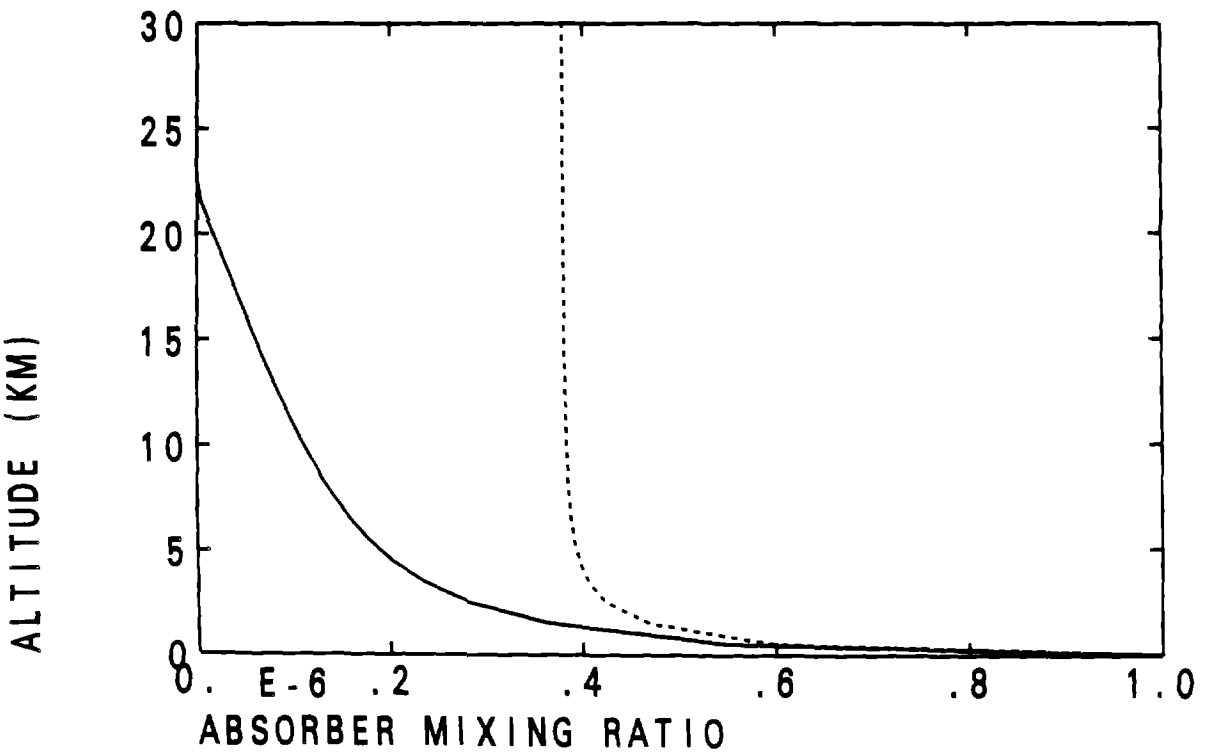
30
25
20
15
10
5
0
ALTITUDE (KM)
0. E-6 .2 .4 .6 .8 1.0
ABSORBER MIXING RATIO

Fig. 12